

Naval Surface Warfare Center

Carderock Division

West Bethesda, MD 20817-5700

NSWCCD-50-TR-2008/035 April 2008

Hydromechanics Department Report

Added Resistance Analytical Tool Evaluation for JHSS

by

Sang Soo Lee

20080811 034



Approved for public release; Distribution is unlimited.

REPORT DOCUMENTATION PAGE

Form Approved
OMB No. 0704-0188

Public reporting burden for this collection of information is estimated to average 1 hour per response, including the time for reviewing instructions, searching existing data sources, gathering and maintaining the data needed, and completing and reviewing this collection of information. Send comments regarding this burden estimate or any other aspect of this collection of information, including suggestions for reducing this burden to Department of Defense, Washington Headquarters Services, Directorate for Information Operations and Reports (0704-0188), 1215 Jefferson Davis Highway, Suite 1204, Arlington, VA 22202-4302. Respondents should be aware that notwithstanding any other provision of law, no person shall be subject to any penalty for failing to comply with a collection of information if it does not display a currently valid OMB control number. **PLEASE DO NOT RETURN YOUR FORM TO THE ABOVE ADDRESS.**

1. REPORT DATE (DD-MM-YYYY) 1-Apr-2008		2. REPORT TYPE Final		3. DATES COVERED (From - To) 1-Jan-2006 - 1-Feb-2008	
4. TITLE AND SUBTITLE Added Resistance Analytical Tool Evaluation for JHSS				5a. CONTRACT NUMBER	
				5b. GRANT NUMBER	
				5c. PROGRAM ELEMENT NUMBER	
6. AUTHOR(S) Sang Soo Lee				5d. PROJECT NUMBER	
				5e. TASK NUMBER	
				5f. WORK UNIT NUMBER 07-1-2125-146	
7. PERFORMING ORGANIZATION NAME(S) AND ADDRESS(ES) AND ADDRESS(ES) Naval Surface Warfare Center Carderock Division Seakeeping Division, Code 5500 9500 Macarthur Boulevard West Bethesda, MD 20817-5700				8. PERFORMING ORGANIZATION REPORT NUMBER NSWCCD-50-TR-2008/035	
9. SPONSORING / MONITORING AGENCY NAME(S) AND ADDRESS(ES) Naval Sea Systems Command PMS 385 1333 Isaac Hull Avenue SE Washington, DC 20376				10. SPONSOR/MONITOR'S ACRONYM(S)	
				11. SPONSOR/MONITOR'S REPORT NUMBER(S)	
12. DISTRIBUTION / AVAILABILITY STATEMENT Approved for public release. Distribution is unlimited					
13. SUPPLEMENTARY NOTES					
14. ABSTRACT Three numerical simulation codes that compute the added resistance in waves, SWAN1, LAMP2 and VERES, are evaluated using model test data of the Joint High Speed Sealift (JHSS). The added resistance tests were conducted with the Model 5633-3 with the scale ratio of 34.121. This model has the JHSS conventional Baseline Shaft and Strut hullform with Gooseneck Bulb. The model was free to heave, pitch and roll. The model tests were conducted in regular head waves at two full-scale ship speeds of 25 and 36 knots, with Froude numbers of 0.24 and 0.35, respectively. The comparison between numerical simulation results and test data show that heave and pitch motions are well predicted by all three codes evaluated. For the added resistance, SWAN1, LAMP2 and VERES produced good agreement with the test data. SWAN1 produced the best predictions for the added resistance as well as the heave and pitch motions.					
15. SUBJECT TERMS Joint High Speed Sealift (JHSS), Added Resistance					
16. SECURITY CLASSIFICATION OF:			17. LIMITATION OF ABSTRACT SAR	18. NUMBER OF PAGES 30	19a. NAME OF RESPONSIBLE PERSON Sang Soo Lee
a. REPORT UNCLASSIFIED	b. ABSTRACT UNCLASSIFIED	c. THIS PAGE UNCLASSIFIED			19b. TELEPHONE NUMBER (include area code) 301-227-6087

This Page Left Intentionally Blank

Contents

	<i>Page</i>
ABSTRACT.....	1
ADMINISTRATIVE INFORMATION	1
INTRODUCTION	1
NUMERICAL CODES EVALUATED	2
SWAN1.....	2
LAMP2	3
VERES.....	3
MODEL TEST RESULTS	4
COMPARISON WITH NUMERICAL SIMULATION RESULTS.....	6
SUMMARY	7
ACKNOWLEDGEMENTS.....	8
REFERENCES	29

Figures

	<i>Page</i>
1. Test conditions when $Fr = 0.24$.	11
2. Test conditions when $Fr = 0.35$.	11
3. Magnitude of heave RAO of JHSS Model 5633-3 in head waves when $Fr = 0.24$.	12
4. Magnitude of heave RAO of JHSS Model 5633-3 in head waves when $Fr = 0.35$.	12
5. Magnitude of pitch RAO of JHSS Model 5633-3 in head waves when $Fr = 0.24$.	13
6. Magnitude of pitch RAO of JHSS Model 5633-3 in head waves when $Fr = 0.35$.	13
7. Normalized added resistance of JHSS Model 5633-3 when $Fr = 0.24$.	14
8. Normalized added resistance of JHSS Model 5633-3 when $Fr = 0.35$.	14
9. Average added resistance of JHSS Model 5633-3 when $Fr = 0.24$.	15
10. Average added resistance of JHSS Model 5633-3 when $Fr = 0.35$.	15
11. Heave and Pitch RAOs from SWAN1 when $Fr = 0.24$ and (sinkage, trim) = (0, 0), (0.2576 m, 0.1 deg), (0.3484 m, 0.2007 deg).	16
12. Heave and Pitch RAOs from SWAN1 when $Fr = 0.35$ and (sinkage, trim) = (0, 0), (0.602 m, 0.23 deg), (0.684 m, 0.4058 deg).	17
13. Normalized added resistance from SWAN1 when $Fr = 0.24$ and 0.35.	18
14. Heave and Pitch RAOs from LAMP2 when $Fr = 0.24$ and wave-height/wave-length = 0.005, 0.01.	19
15. Heave and Pitch RAOs from LAMP2 when $Fr = 0.35$ and wave-height/wave-length = 0.005, 0.01.	20
16. Normalized added resistance from LAMP2 when $Fr = 0.24$ and 0.35, and wave-height/wave-length = 0.005, 0.01.	21
17. Heave and Pitch RAOs from VERES when $Fr = 0.24$ using different calculation methods.	22
18. Heave and Pitch RAOs from VERES when $Fr = 0.35$ using different calculation methods.	23
19. Normalized added resistance from VERES when $Fr = 0.24$ and 0.35 using different calculation methods.	24
20. Comparison of Heave and Pitch RAOs between numerical predictions and model test data when $Fr = 0.24$.	25
21. Comparison of Heave and Pitch RAOs between numerical predictions and model test data when $Fr = 0.35$.	26
22. Comparison of normalized added resistance between numerical predictions and model test data when $Fr = 0.24$ and 0.35.	27

Tables

	<i>Page</i>
1. Test results of JHSS Model 5633-3 in head regular waves when $Fr = 0.24$ (model scale).	9
2. Test results of JHSS Model 5633-3 in head regular waves when $Fr = 0.35$ (model scale).	10

This Page Left Intentionally Blank

ABSTRACT

Three numerical simulation codes that compute the added resistance in waves, SWAN1, LAMP2 and VERES, are evaluated using model test data of the Joint High Speed Sealift (JHSS).

The added resistance tests were conducted with the Model 5633-3 with the scale ratio of 34.121. This model has the JHSS conventional Baseline Shaft and Strut hullform with Gooseneck Bulb. The model was free to heave, pitch and roll. The model tests were conducted in regular head waves at two full-scale ship speeds of 25 and 36 knots, with Froude numbers of 0.24 and 0.35, respectively.

The comparison between numerical simulation results and test data show that heave and pitch motions are well predicted by all three codes evaluated. For the added resistance, SWAN1, LAMP2 and VERES produced good agreement with the test data. SWAN1 produced the best predictions for the added resistance as well as the heave and pitch motions.

ADMINISTRATIVE INFORMATION

This work was funded by the Joint High Speed Sealift (JHSS) program office, NAVSEA PMS 385. This work was performed by the Seakeeping Division Code 5500 of the Naval Surface Warfare Center, Carderock Division (NSWCCD) under work unit numbers 07-1-2125-146 and 08-1-2125-146.

INTRODUCTION

As a part of the High Speed Sealift Development Program [1]*, the numerical simulation tools that can compute the added resistance in waves are evaluated using model test data of the Joint High Speed Sealift (JHSS). The added resistance in waves is defined as the difference between the time-average resistance in waves and the calm-water resistance at the same ship speed. The information about the added resistance is important to estimate the reserve power requirements for high speed ships in a sea state in severe weather.

There are many causes that contribute to the added resistance [2]. Vossers [3] and Hanaoka et al. [4] suggested that there were three main components in the resistance of a ship in waves. These are the interference between incident waves and waves generated by ship motions, the wave reflection against the ship, and a damping force. The damping force could be measured by an experiment with forced/prescribed heaving and pitching motions in calm water. In general, the resistance force due to the wave interaction is the largest contributor to the added resistance.

* References given on page 29.

Several theoretical approaches exist to compute the added resistance [5 -13]. A good summary of various theoretical approaches can be found in Strom-Tejsen et al. [2]. One conclusion that can be drawn from these analyses is that added resistance is proportional to the square of the incident wave height. These theoretical analyses also show that the added resistance is dependent on the ship motions and their phase relationship to the wave field. The added resistance in a seaway is independent of calm-water resistance. It is also believed that added resistance can be considered as a nonviscous phenomenon and therefore can be determined by inertial and wave effects.

In this report, various added resistance simulation codes including SWAN1, LAMP2 and VERES were used to compare with the model test data. Only the head sea condition was considered since it usually produced the maximum added resistance. Model tests were conducted with the Model 5633-3 with the Joint High Speed Sealift (JHSS) conventional Baseline Shaft and Strut (BSS) hullform and Gooseneck Bulb (GB). The model was restrained in surge, sway and yaw motions, but was free to heave, pitch and roll. The full-scale speeds of 25 and 36 knots, with Froude numbers of 0.24 and 0.35, respectively, were tested.

NUMERICAL CODES EVALUATED

SWAN1

SWAN1 (Ship Wave ANalysis) [14] is a hydrodynamics program that computes the steady and unsteady flow solutions around a single-hull ship. It is a potential flow solver of the linear steady and time-harmonic free-surface flow around a ship. The ship can move with a constant forward speed in clam water and in waves. SWAN1 computes the flow properties inside the fluid domain, over the hull and on the free surface. Integrated hydrodynamic forces acting on the vessel are also computed by pressure integration over the hull as well as momentum analysis. It uses a three-dimensional Rankine panel method. Panels are distributed on the ship hull and part of the free surface. The use of the Rankine source as the Green function, combined with an iterative method for the solution of the resulting linear systems, leads to the efficient solution of the seakeeping problems. The ship wave resistance is determined by a wake analysis, which evaluates the momentum deficit in the Kelvin wake. Flat plate friction resistance and form resistance are not evaluated by SWAN1.

SWAN1 requires two mandatory input files. The first one specifies the ship geometry as a set of offsets. Bilge keels and skeg can be included at each station. The other input file defines job control parameters such as ship speed, wave headings, frequencies, ship inertia, etc. SWAN1 produces a free surface, wake sheet, and hull mesh automatically from the hull offsets.

The lower limit of the ship speed is subject to the numerical stability constraint. As speed decreases, short wavelengths in the wave pattern become more pronounced and the panel size must become smaller. The lower limit of SWAN1 simulation is set at $Fr = 0.1$ and the upper limit of the ship speed is set at $Fr = 1.5$.

LAMP2

LAMP is the SAIC three-dimensional time-domain Large-Amplitude Motions Program [15]. It calculates time-domain motions and loads of floating bodies with or without forward speed using 3-D potential flow panel method. The hydrodynamic solution computes the combined effect of forward speed, body motion (*i.e.* the radiation problem), and the interaction with the incident wave (*i.e.* the diffraction problem) using a choice of singularity models and computational approaches.

In LAMP2, the 3-D body-linear approach is used to compute the hydrodynamic part of the pressure forces. It uses the free surface boundary conditions on the mean water surface. Meanwhile, the hydrostatic restoring force and the Froude-Krylov wave force are calculated on the actual hull surface below the incident wave surface.

LAMP uses a straightforward time stepping procedure in which all forces acting on the body are computed at each time step for the actual ship position and motion history. The position and velocity of the ship are updated by integrating the equations of motions in the time domain.

Viscous effects are not included in this potential flow solver, although they are included as external forces in the overall force calculation. Semi-empirical formulations or user specified coefficients are used for the viscous forces.

The added resistance is calculated from the time dependent surge forces obtained from LAMP2 simulations. It is obtained as the difference between the average surge force in waves and the calm-water resistance at the same ship speed.

VERES

The ShipX Vessel Response Plug-In is a ShipX implementation of the Vessel RESponse program (VERES) [16, 17]. ShipX is Marintek's common platform for ship design analyses. VERES is based on linear potential theory. The theory is developed for moderate wave heights inducing moderate motions on a slender ship. The hull is defined by a set of body lines at freely selected longitudinal positions. The cross-sections of the hull are specified by a number of offset points.

VERES can be applied on mono-hull and multi-hull vessels at low as well as high speed. At low and moderate speeds, Froude numbers up to 0.25 – 0.30, the problem is solved by traditional strip theory developed by Salvesen, Tuck & Faltinsen [18]. At higher speeds, Froude numbers larger than approximately 0.4, the high speed formulation developed by Faltinsen & Zhao [19] is used. The interaction from the strips upstream is considered in the high speed theory. Since the higher Froude number of the model test is 0.35, both strip-theory and high-speed formulations will be evaluated in this report.

When the traditional strip theory is used, the exciting forces and hydrodynamic forces can be calculated using the strip theory approach. VERES can also use the direct pressure integration method that divides the hull into panels and applies the pressure components at each panel to compute the exciting and hydrodynamic forces.

There are two options in added resistance computation. The user can choose the Gerritsma and Beukelman [10] method or direct pressure integration method. According to the former

method, that uses the slender body theory, the added resistance is strongly dependent on the relative vertical motion between the ship and waves.

MODEL TEST RESULTS

The added resistance tests were conducted with the Model 5633-3. This model has the Joint High Speed Sealift (JHSS) conventional Baseline Shaft and Strut (BSS) hullform with Gooseneck Bulb (GB). A detailed description of the model can be found in Cusanelli [20] and Cusanelli & Chesnakas [21]. The LBP of the full-scale ship is 950.5 ft (289.7 m) and that of the model is 27.857 ft (8.491 m) and the scale ratio is 34.121.

The tests were carried out at NSWCCD in the Deep Water Basin (Carriage 2). The model was restrained in surge, sway and yaw motions, but was free to heave, pitch and roll. The model was attached to the carriage towing girder using two linear bearing floating platform ‘Cusanelli’ tow posts [22] at forward and aft positions. Double-axis gimbal assemblies were used to connect the tow posts and the model. They were mounted on two linear glide rails that were locked in a single longitudinal position throughout the testing. Primary drag force was measured at the forward tow post using a DTMB 4-inch block gauge of 100 lbf capacity. A secondary drag force measurement was made at the aft post using a 4-inch block gauge of 50 lbf capacity. During testing, the second drag gauge was allowed to ‘float’ so as to impart minimal forces on the model. Details of the experimental setup and instruments were described in Cusanelli [23].

The full-scale speeds of 25 and 36 knots, with Froude numbers of 0.24 and 0.35, respectively, were tested in regular head waves. The model was towed at constant speeds of 4.28 and 6.16 knots, respectively. Although the model was allowed to roll, the measured roll angles were very small in the head seas tested.

Since added resistance is the difference between the mean total drag in waves and the calm water drag, accurate measurements of drag in calm water and in waves are needed. Obtaining accurate experimental data on added resistance is difficult because of the small drag increments to be measured. The added resistance depends on the square of the incoming wave amplitude.

In order to compute the resistance in waves, the data are analyzed over a time interval corresponding to an integer number of wave encounter cycles [13]. This was necessary because the linear oscillatory part of the surge exciting force is larger in amplitude than the mean added resistance. Therefore, taking an average of the drag signal over a fraction of a cycle of the oscillation would seriously bias the estimate of the mean value.

Added resistance experiments were carried out over a range of frequencies or wavelengths. A number of runs were selected with different wave heights to determine if the mean added resistance did, in fact, vary with the square of wave amplitude. All tests were conducted in head seas at two ship speeds.

Summary of the test results are given in Tables 1 and 2 for Froude numbers of 0.24 and 0.35, respectively. A spot number (denoted as SpotNo in tables), along with test number (TestNo), was assigned to each test. Only a middle portion of the time-series data was used for the Fourier series analysis and the actual number of cycles used for the analysis was given in the third column (Ncyc). Measured average speed (AvSpeed) and its corresponding Froude number (FrNo) was given in the fourth and fifth columns. The wave height $2A$ (WaveHt), encounter

frequency ω_e (EnOme), frequency ω (Omega), wave length λ (Lamdba), wave number k (WavNum), ratio of the wave-height/wave-length $2A/\lambda$ (wh/Lam), ratio of the wave-length/LBP λ/LBP (Lam/LBP), average total drag (AvgDrag), normalized added resistance (NormAddRes), magnitude of the heave RAO and magnitude of the pitch RAO were tabulated for all test conditions.

The normalized added resistance is defined as

$$\frac{R_a}{\rho g A^2 B^2 / LBP}, \quad (1)$$

where R_a is the average added resistance that is equal to the mean total resistance minus calm water resistance and A is the amplitude of the incoming wave. The ship length, LBP and the beam, B were used in this normalization.

The magnitude of the heave RAO is normalized using the amplitude of the incoming wave A , and the magnitude of the pitch RAO is normalized using kA , i.e.

$$\frac{\eta_3}{A} \quad \text{and} \quad \frac{\eta_5}{kA}. \quad (2)$$

The model test conditions are plotted in Figures 1 and 2, for the Froude numbers 0.24 and 0.35, respectively. The Spot numbers that are given in the second columns in Tables 1 and 2 are written next to the symbols for convenience. As shown in these figures, various wave-length/LBP values were tested while the ratios of the wave-height/wave-length were kept around 0.013. Meanwhile, the effect of the incoming wave amplitudes was investigated at the fixed λ/LBP ratios of 0.9 and 1 when the Froude numbers were 0.24 and 0.35, respectively.

The magnitudes of the heave and pitch RAOs are shown in Figures 3 – 6. The ratio of the wave-height/wave-length of the corresponding test points are plotted in the bottom figures in order to show the effect of the incoming wave amplitude. The results at $\lambda/LBP = 0.9$ and 1 for the Froude numbers of 0.24 and 0.35, respectively, indicate that the heave and pitch RAOs are slightly dependent on the incoming wave amplitude A . The values of the heave and pitch RAOs varied by about 10 % and 20 %, respectively, when $2A/\lambda$ varied from 0.005 to 0.02 in these model tests.

The normalized added resistance, plotted in Figures 7 and 8, show that the added resistance may not vary with the square of wave amplitude. However, the limited data sets of this test did not allow the prediction of any conclusive functional dependency. More accurate measurements of the drag and wave amplitude are necessary since the measured values of the added resistance are relatively small. Figures 9 and 10 show the added resistance (in lbf). In order to calculate the added resistance, the calm water resistance of 17.198 lbf and 35.238 lbf for the Froude numbers of 0.24 and 0.35, respectively, were subtracted from the total average drag. It is shown that the added resistances are indeed very small especially when the incoming wave amplitudes are

small. Although the experimental results by Strom-Tejsen et al. [2] suggest that the linear relationship between the added resistance and wave-amplitude square can be considered a good approximation, the exact correlation may be dependent on the geometry of the ship hulls.

Test results in Figures 7 and 8 show that the maximum added resistance occurs when the ratio of wave-length/LBP is about 1 for Froude number of 0.35 and when the ratio is between 0.85 – 1 for Froude number of 0.24. The values of the normalized added resistance for the high speed are larger than those of the lower ship speed as expected. It is believed that the normalized added resistance has a maximum value when the wave length is of the order of the ship length and that the maximum added resistance occurs when the relative vertical motion between the ship and the waves is large [24].

COMPARISON WITH NUMERICAL SIMULATION RESULTS

In this section, the model test data will be compared with the simulation results from SWAN1, LAMP2 and VERES. Only the test data with ratios of the wave-height/wave-length of about 0.013 will be used for comparisons. The heave and pitch RAOs are normalized by A and kA , respectively, and the added resistance was normalized using Equation (1) given in the previous section.

Figures 11 – 13 show the comparison between the test data and the numerical simulation results from SWAN1. The experimental data were plotted using symbols (black dots) and the numerical results were plotted using solid lines. As shown in the bottom of Figure 13, the ratio of wave-height/wave-length of the corresponding experimental data was about 0.013. The effect of sinkage and trim condition was investigated by using three different values for SWAN1 calculations. The sinkage and trim values from the test data are 0.2576 m and 0.1 degrees for the 25 knot test and 0.602 m and 0.23 degrees for the 36 knot one, where positive trim value represents the bow-down condition. The other nonzero sinkage and trim values in SWAN1 simulation were obtained from the steady calculations of SWAN1.

When the Froude number is 0.24, different sinkage and trim values do not affect the heave and pitch motions as well as the added resistance. However, the peak values and peak locations of the heave and pitch motions and the added resistance are dependent on the sinkage and trim values in the high speed case when the Froude number is 0.35.

It is shown in Figures 11 and 12 that the pitch RAOs from SWAN1 prediction with the sinkage and trim values of the test data have good agreement with the experimental results at both speeds. However, SWAN1 over-predicted the magnitude of the heave RAO, especially the maximum values. As shown in Figure 13, SWAN1 under-predicted the normalized added resistance at both speeds. Meanwhile, the peak location of the added resistance from the SWAN1 occurs at larger wave-length/LBP value when the Froude number was 0.35.

Figures 14 – 16 show the results from LAMP2 predictions. In order to investigate the effect of the wave amplitude in the LAMP2 calculations, two different values of the incoming wave amplitudes were used with the wave-height to wave-length ratios of 0.005 and 0.01. It is shown that the difference in the wave amplitude does not affect the heave and pitch motions as well as the added resistance. Comparison with the model test data show that LAMP2 over-predicted the

heave and pitch motions at both speeds. Meanwhile, LAMP2 under-predicted the normalized added resistance.

Figures 17 and 18 show the heave and pitch motions from VERES predictions using different calculation methods. 'Strip-Strip' denotes the case when the strip-theory formulation is used and the strip theory is applied to compute the exciting forces and hydrodynamic forces. 'Strip-Pressure' denotes the case when the pressure integration is used for the exciting and hydrodynamic force calculations along with the strip-theory formulation. The high-speed formulation is denoted by 'High-Pressure'. The 'High-Pressure' method, that uses the high-speed formulation with the pressure integration for the forces, produces larger magnitude of the heave and pitch RAOs compared to the other two methods. VERES user's manual recommends to use strip-theory formulation for Froude numbers up to 0.25 – 0.30 and high speed formulation for Froude numbers larger than 0.4. The results in Figures 17 and 18 indicate that the strip-theory formulation predicts better for the Froude numbers tested.

Since there are two options to compute the added resistance, there are five combinations of methods for the added resistance predictions in VERES. As shown in Figure 19, the peak values of the normalized added resistance using different methods are varying widely. It is shown that the 'Strip-Pressure-GB' method, that uses the strip-theory formulation, pressure integration for the forces and Gerritsma and Beukelman's added resistance calculation, produces the best agreement with the measured heave, pitch motions and added resistance.

The comparison between the model test data and numerically predicted results from all three simulation codes are summarized in Figures 20 – 22. The results from SWAN1 calculations using the sinkage and trim values obtained from the test data, LAMP2 predictions with the wave-height to wave-length ratios of 0.01, and VERES using the 'Strip-Pressure-GB' method predictions were plotted using green, blue and red lines, respectively. It is shown in Figures 20 and 21 that the predicted heave and pitch motions using different numerical prediction codes are in good agreement. The magnitude of the heave RAO was slightly over-predicted by most of the prediction codes. The magnitude of the pitch RAO was well predicted by all numerical codes.

Figure 22 shows that SWAN1 produces the best prediction of the model test data for the normalized added resistance. Although the results from VERES appear closer to the test data, it must be noted that only the best match VERES results, among many other available methods, are presented in this figure. The added resistance from LAMP2 prediction was lower than the test data at both ship speeds.

It can be summarized that SWAN1 produces the best predictions for the added resistance as well as the heave and pitch motions. The other codes, LAMP2 and VERES also produced reasonably good comparisons.

SUMMARY

The model test data were compared with SWAN1, LAMP2 and VERES simulation results. The added resistance tests were conducted with the Model 5633-3 that has the Joint High Speed Sealift (JHSS) conventional Baseline Shaft and Strut (BSS) hull form with Gooseneck Bulb (GB). During the test on Carriage 2, the model was restrained in surge, yaw and sway motions, but was free to heave, pitch and roll. Two ship speeds with Froude numbers of 0.24 and 0.35 were tested in regular head waves.

The comparison between test data and numerical simulation results show that heave and pitch motions are well predicted by all three codes investigated. For the added resistance, SWAN1, LAMP2 and VERES produced good agreement with the test data. SWAN1 produced the best predictions for the added resistance as well as the heave and pitch motions.

ACKNOWLEDGEMENTS

The author is very grateful to D. S. Cusanelli and B. Metcalf of the Resistance & Propulsion Division (Code 5800) for conducting experiments. Thanks are also due to A. Silver for helpful discussions.

Table 1. Test results of JHSS Model 5633-3 in head regular waves when $Fr = 0.24$ (model scale).

TestNo	SpotNo	Ncyc	AvSpeed	FrNo	WaveHt	EnOme	Omega	Lambda	WavNum	wh/Lam	Lam/LBP	AvgDrag	NormAddRes	HEAVE	PITCH/kA
...	knots	...	ft	rad/s	rad/s	ft	rad/ft		...	lbf	...	TrFn_amp	TrFn_amp
59	225	20	4.30	0.242	0.286	5.200	3.072	21.416	0.293	0.0134	0.769	19.84	6.083	0.526	0.266
59	173	24	4.29	0.242	0.307	4.931	2.959	23.090	0.272	0.0133	0.829	20.67	6.982	0.646	0.370
59	167	12	4.30	0.242	0.284	4.928	2.957	23.116	0.272	0.0123	0.830	20.36	7.421	0.668	0.381
59	170	25	4.29	0.242	0.285	4.927	2.957	23.115	0.272	0.0123	0.830	20.37	7.379	0.646	0.372
59	204	31	4.29	0.242	0.318	4.784	2.895	24.116	0.261	0.0132	0.866	21.60	8.221	0.713	0.449
59	201	32	4.29	0.242	0.307	4.780	2.894	24.138	0.260	0.0127	0.867	21.20	8.029	0.710	0.452
59	198	12	4.29	0.242	0.328	4.775	2.892	24.165	0.260	0.0136	0.868	21.84	8.177	0.717	0.448
59	179	16	4.30	0.242	0.333	4.644	2.834	25.172	0.250	0.0132	0.904	21.84	7.931	0.770	0.505
59	176	22	4.29	0.242	0.303	4.641	2.833	25.174	0.250	0.0120	0.904	21.30	8.445	0.764	0.506
59	229	35	4.30	0.242	0.155	4.637	2.830	25.230	0.249	0.0062	0.906	18.37	9.173	0.767	0.453
59	228	19	4.30	0.242	0.154	4.632	2.828	25.264	0.249	0.0061	0.907	18.51	10.493	0.769	0.416
59	194	26	4.30	0.242	0.345	4.500	2.770	26.341	0.239	0.0131	0.946	22.19	7.933	0.754	0.562
59	191	26	4.29	0.242	0.331	4.490	2.766	26.412	0.238	0.0125	0.948	22.04	8.352	0.741	0.560
59	213	26	4.30	0.242	0.369	4.351	2.703	27.661	0.227	0.0133	0.993	22.98	8.043	0.778	0.630
59	216	19	4.30	0.243	0.363	4.334	2.695	27.825	0.226	0.0131	0.999	23.12	8.482	0.773	0.628
59	182	14	4.29	0.242	0.412	4.221	2.645	28.890	0.218	0.0143	1.037	24.30	7.903	0.783	0.692
59	185	25	4.29	0.242	0.382	4.216	2.642	28.937	0.217	0.0132	1.039	23.00	7.529	0.759	0.681
59	188	26	4.29	0.242	0.370	4.213	2.641	28.972	0.217	0.0128	1.040	22.56	7.415	0.784	0.672
59	210	22	4.30	0.242	0.435	3.933	2.511	32.032	0.196	0.0136	1.150	23.22	6.027	0.745	0.744
59	207	19	4.30	0.242	0.446	3.926	2.507	32.120	0.196	0.0139	1.153	24.08	6.532	0.770	0.773
59	222	13	4.30	0.242	0.438	3.681	2.391	35.296	0.178	0.0124	1.267	22.81	5.516	0.796	0.848
59	219	18	4.30	0.242	0.400	3.678	2.389	35.345	0.178	0.0113	1.269	21.74	5.362	0.776	0.841
60	241	31	4.30	0.242	0.423	4.649	2.836	25.135	0.250	0.0168	0.902	24.51	7.747	0.747	0.497
60	232	30	4.30	0.242	0.167	4.642	2.832	25.193	0.249	0.0066	0.904	18.67	10.002	0.759	0.448
60	234	40	4.30	0.242	0.243	4.640	2.832	25.197	0.249	0.0096	0.905	19.95	8.811	0.761	0.486
60	238	51	4.29	0.242	0.340	4.638	2.832	25.205	0.249	0.0135	0.905	22.02	7.868	0.755	0.494
60	235	49	4.30	0.242	0.249	4.638	2.831	25.217	0.249	0.0099	0.905	20.02	8.608	0.770	0.486
60	242	51	4.29	0.242	0.428	4.637	2.831	25.217	0.249	0.0170	0.905	24.76	7.793	0.730	0.504
60	237	29	4.30	0.242	0.337	4.637	2.831	25.219	0.249	0.0134	0.905	21.82	7.698	0.726	0.493
60	231	17	4.30	0.242	0.168	4.638	2.831	25.224	0.249	0.0067	0.906	18.86	11.067	0.798	0.466
60	263	41	4.30	0.242	0.204	4.634	2.830	25.245	0.249	0.0081	0.906	19.32	9.692	0.728	0.459
60	262	45	4.29	0.242	0.201	4.631	2.828	25.267	0.249	0.0080	0.907	19.35	10.014	0.777	0.445

Table 2. Test results of JHSS Model 5633-3 in head regular waves when $Fr = 0.35$ (model scale).

TestNo	SpotNo	Ncyc	AvSpeed	FrNo	WaveHt	EnOme	Omega	Lambda	WavNum	wh/Lam	Lam/LBP	AvgDrag	NormAddRes	HEAVE	PITCH/KA
...	knots	...	ft	rad/s	rad/s	ft	rad/ft		...	lbf	...	TrFn_amp	TrFn_amp
59	226	24	6.19	0.349	0.263	6.108	3.063	21.548	0.292	0.0122	0.774	37.45	6.055	0.304	0.166
59	174	17	6.18	0.348	0.315	5.799	2.960	23.075	0.272	0.0137	0.828	38.24	5.713	0.512	0.248
59	168	48	6.18	0.348	0.290	5.799	2.960	23.081	0.272	0.0125	0.829	37.78	5.733	0.506	0.245
59	171	38	6.18	0.348	0.302	5.795	2.958	23.094	0.272	0.0131	0.829	37.96	5.650	0.498	0.251
59	199	38	6.18	0.348	0.323	5.614	2.896	24.105	0.261	0.0134	0.865	39.67	8.040	0.641	0.328
59	202	45	6.18	0.348	0.314	5.613	2.895	24.113	0.261	0.0130	0.866	38.95	7.144	0.635	0.323
59	205	32	6.18	0.349	0.324	5.606	2.892	24.159	0.260	0.0134	0.867	39.52	7.698	0.642	0.324
59	177	27	6.18	0.349	0.311	5.447	2.837	25.110	0.250	0.0124	0.901	39.68	8.710	0.755	0.383
59	180	21	6.18	0.348	0.344	5.440	2.835	25.145	0.250	0.0137	0.903	40.68	8.677	0.760	0.381
59	195	23	6.18	0.349	0.344	5.256	2.769	26.360	0.238	0.0131	0.946	42.04	10.845	0.913	0.488
59	192	19	6.18	0.349	0.331	5.254	2.768	26.378	0.238	0.0126	0.947	41.76	11.239	0.914	0.484
59	214	23	6.18	0.349	0.371	5.075	2.704	27.647	0.227	0.0134	0.992	43.76	11.705	1.011	0.584
59	217	44	6.19	0.349	0.366	5.062	2.698	27.755	0.226	0.0132	0.996	43.60	11.776	1.022	0.589
59	189	19	6.18	0.349	0.377	4.914	2.645	28.887	0.218	0.0131	1.037	44.24	11.955	1.107	0.648
59	183	20	6.18	0.348	0.424	4.907	2.643	28.930	0.217	0.0147	1.039	46.58	11.941	1.071	0.655
59	186	19	6.18	0.349	0.393	4.906	2.642	28.948	0.217	0.0136	1.039	44.51	11.350	1.065	0.655
59	208	33	6.18	0.349	0.451	4.553	2.509	32.085	0.196	0.0141	1.152	47.08	11.019	1.154	0.826
59	211	33	6.18	0.349	0.425	4.553	2.509	32.089	0.196	0.0132	1.152	46.04	11.318	1.124	0.834
59	220	26	6.18	0.349	0.405	4.245	2.389	35.349	0.178	0.0115	1.269	43.30	9.283	1.132	0.948
59	223	12	6.18	0.349	0.451	4.243	2.389	35.362	0.178	0.0128	1.269	44.80	8.888	1.112	0.936
60	245	17	6.18	0.349	0.169	5.107	2.715	27.418	0.229	0.0062	0.984	36.82	10.488	1.033	0.505
60	257	36	6.18	0.349	0.266	5.089	2.708	27.553	0.228	0.0096	0.989	40.39	13.793	1.059	0.556
60	248	16	6.19	0.349	0.169	5.089	2.708	27.556	0.228	0.0061	0.989	37.00	11.639	1.000	0.530
60	251	21	6.19	0.349	0.202	5.089	2.708	27.562	0.228	0.0073	0.989	38.08	13.132	1.057	0.503
60	250	11	6.19	0.349	0.194	5.088	2.708	27.565	0.228	0.0070	0.990	37.81	12.889	1.068	0.541
60	247	26	6.19	0.349	0.169	5.088	2.707	27.569	0.228	0.0061	0.990	37.18	12.922	1.024	0.518
60	244	15	6.19	0.349	0.165	5.086	2.707	27.579	0.228	0.0060	0.990	36.81	10.979	1.032	0.513
60	260	33	6.18	0.349	0.367	5.081	2.705	27.609	0.228	0.0133	0.991	43.63	11.760	1.016	0.550
60	253	18	6.18	0.349	0.170	5.079	2.705	27.618	0.228	0.0062	0.991	37.50	14.783	1.064	0.534
60	259	36	6.19	0.349	0.358	5.080	2.705	27.619	0.228	0.0130	0.991	43.95	12.872	1.010	0.572
60	256	33	6.18	0.349	0.262	5.079	2.705	27.623	0.228	0.0095	0.992	40.22	13.736	1.055	0.549
60	254	12	6.18	0.349	0.173	5.076	2.704	27.641	0.227	0.0063	0.992	37.72	15.658	1.082	0.554

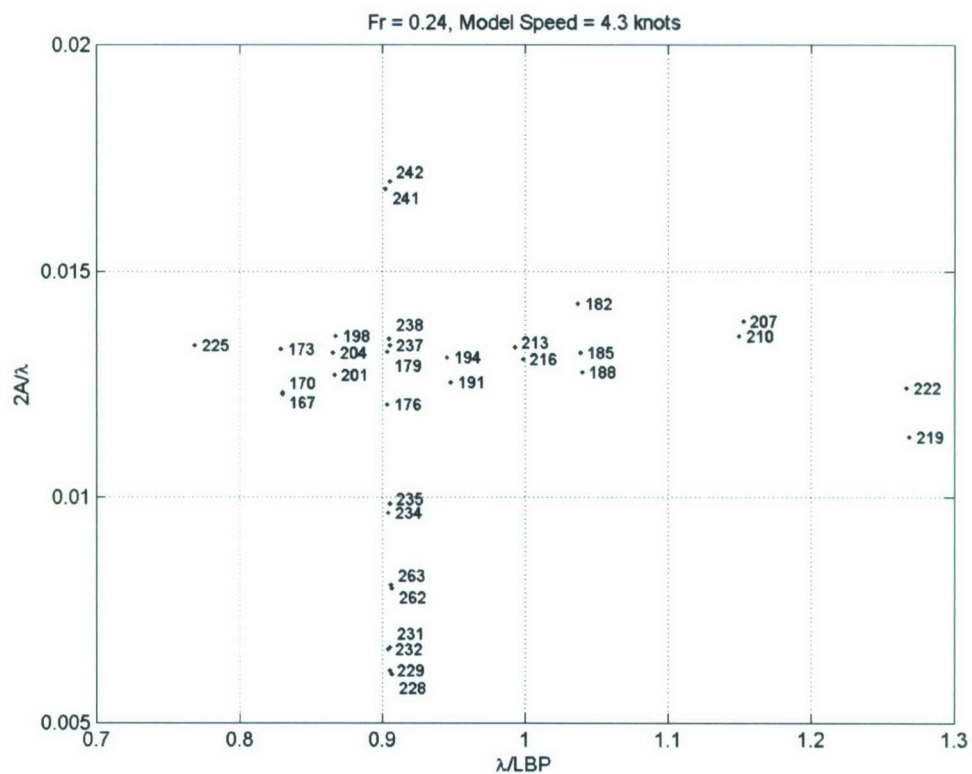


Figure 1. Test conditions when Fr = 0.24.

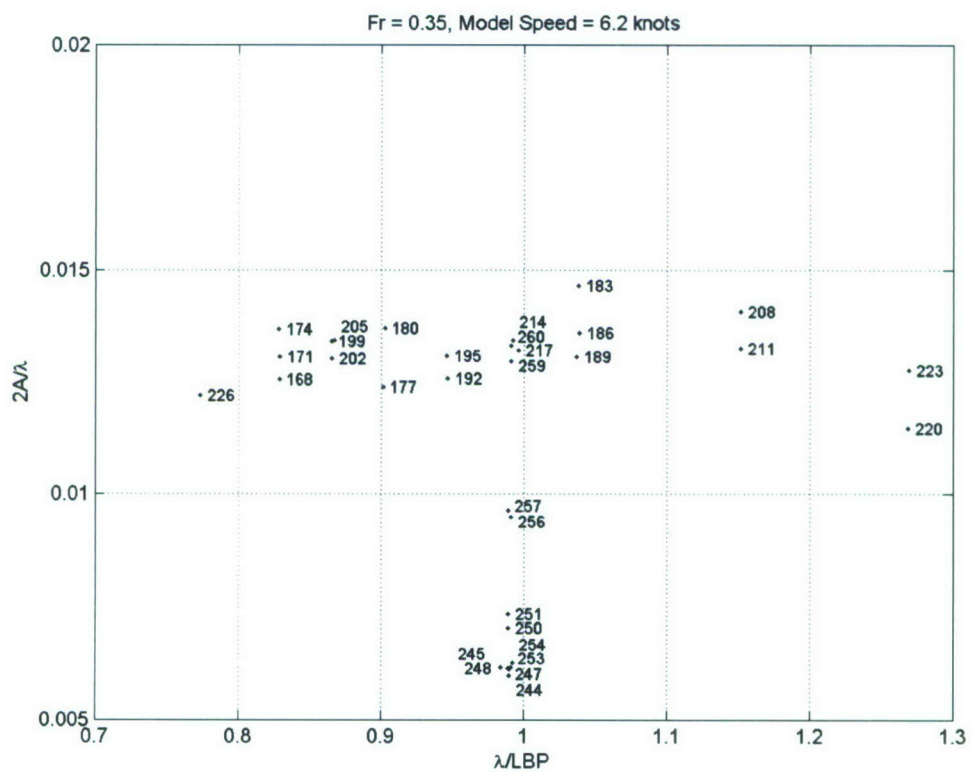


Figure 2. Test conditions when Fr = 0.35.

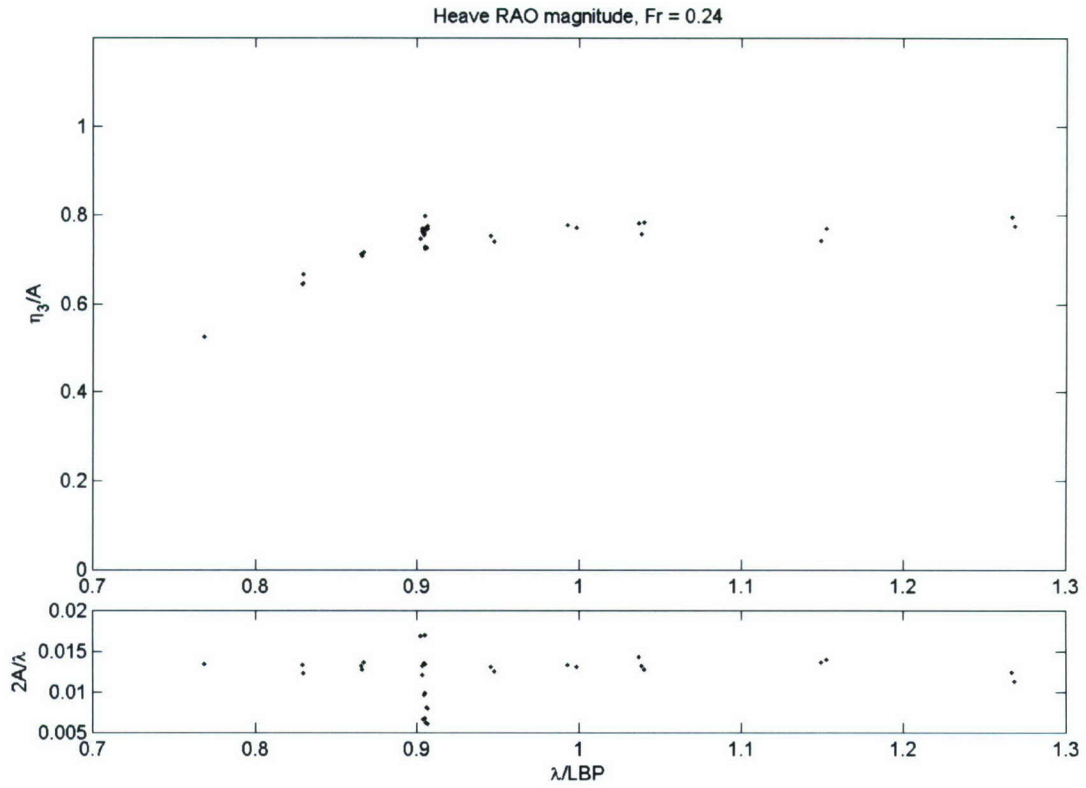


Figure 3. Magnitude of heave RAO of JHSS Model 5633-3 in head waves when Fr = 0.24.

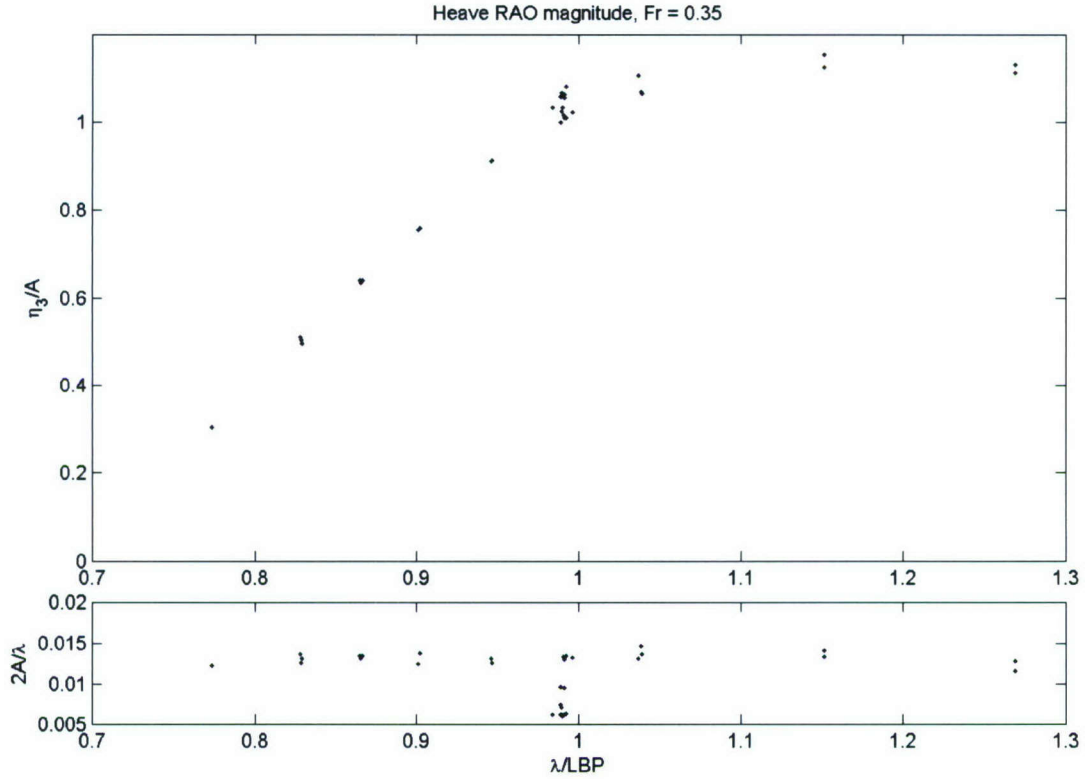


Figure 4. Magnitude of heave RAO of JHSS Model 5633-3 in head waves when Fr = 0.35.

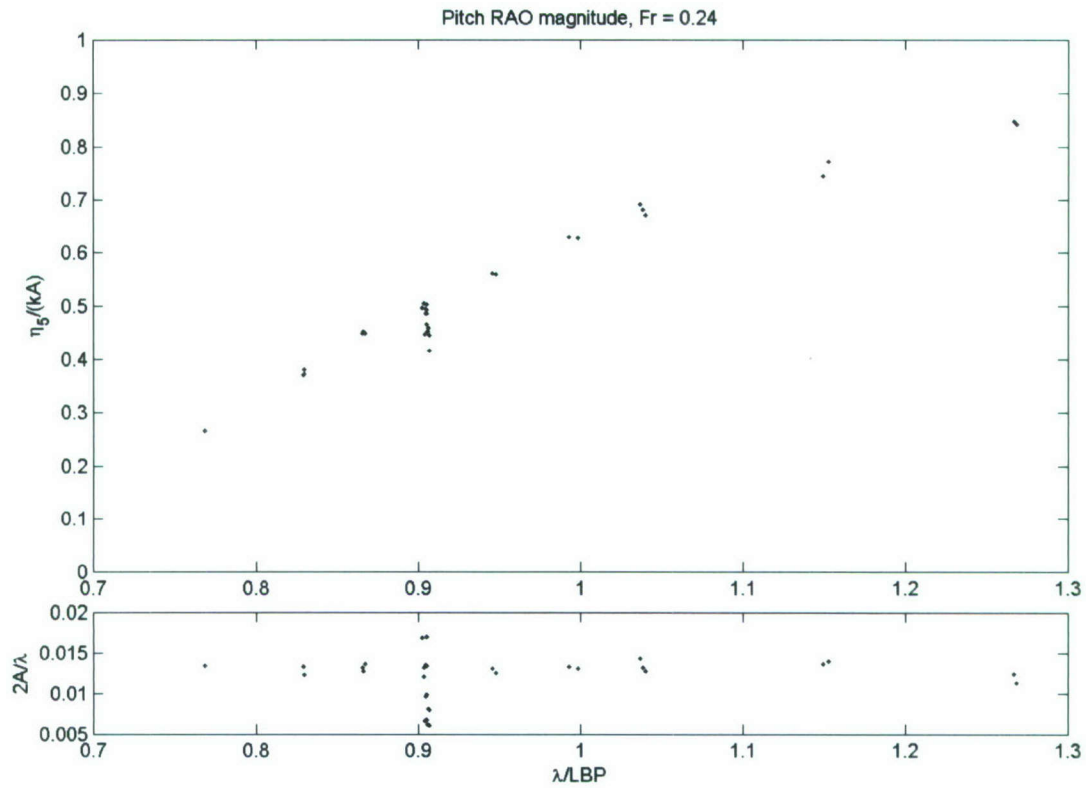


Figure 5. Magnitude of pitch RAO of JHSS Model 5633-3 in head waves when $Fr = 0.24$.

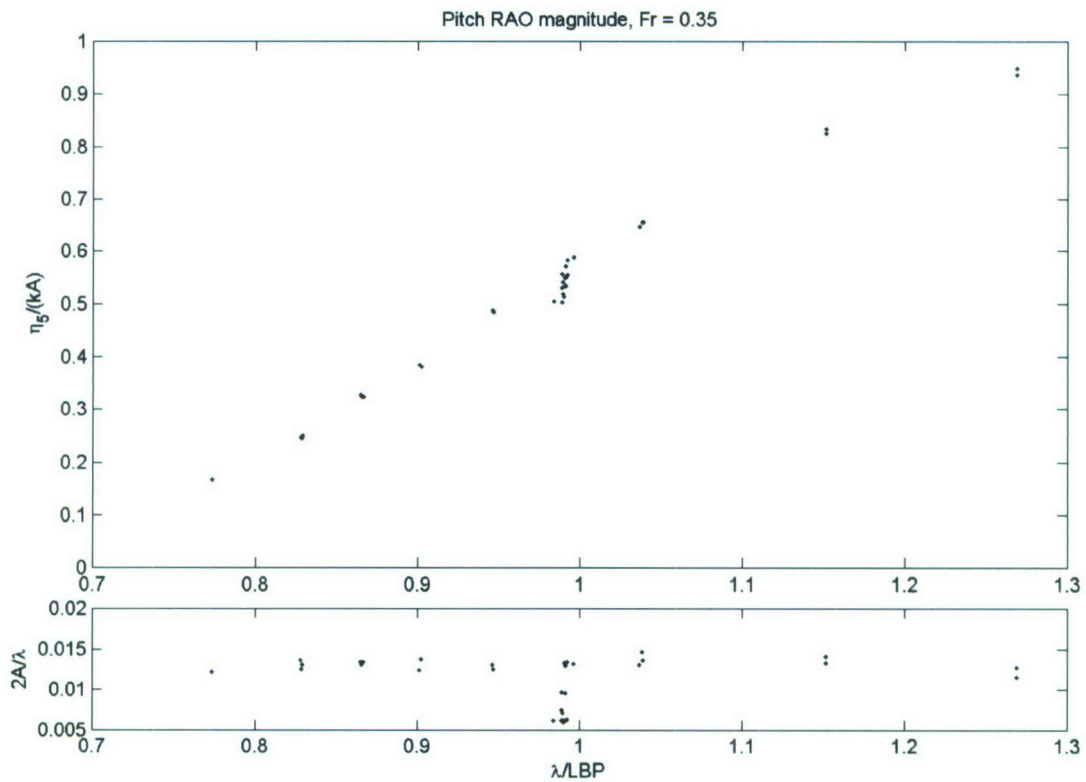


Figure 6. Magnitude of pitch RAO of JHSS Model 5633-3 in head waves when $Fr = 0.35$.

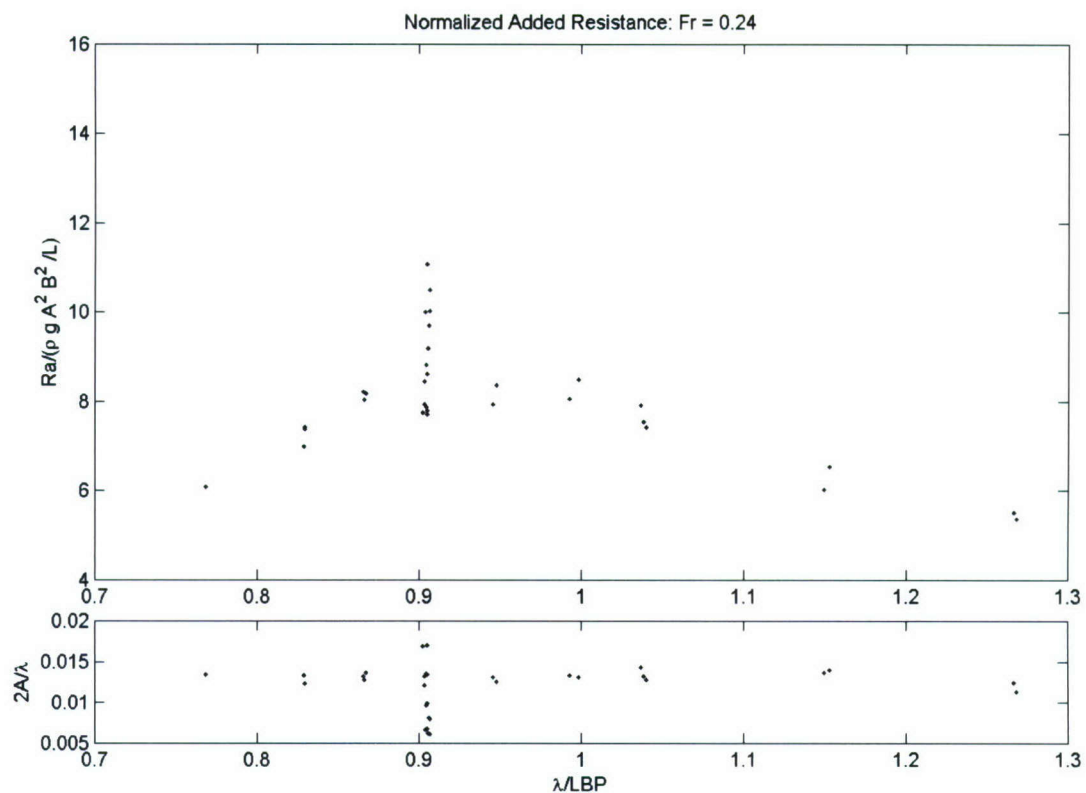


Figure 7. Normalized added resistance of JHSS Model 5633-3 when $Fr = 0.24$.

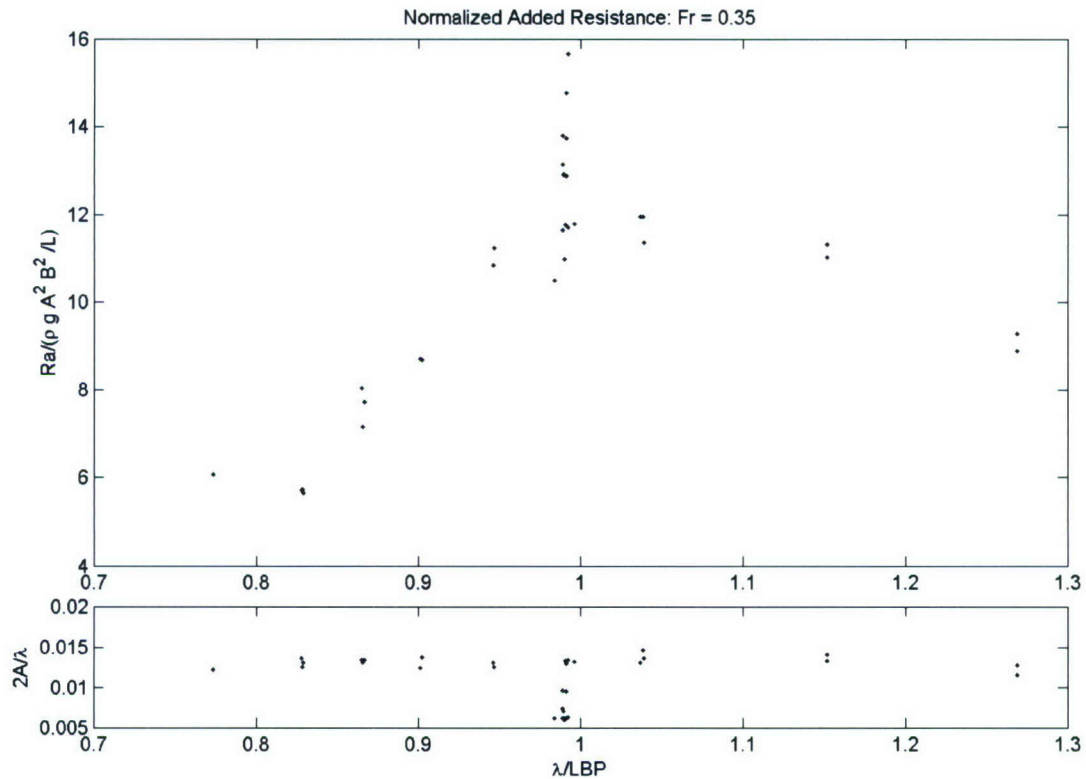


Figure 8. Normalized added resistance of JHSS Model 5633-3 when $Fr = 0.35$.

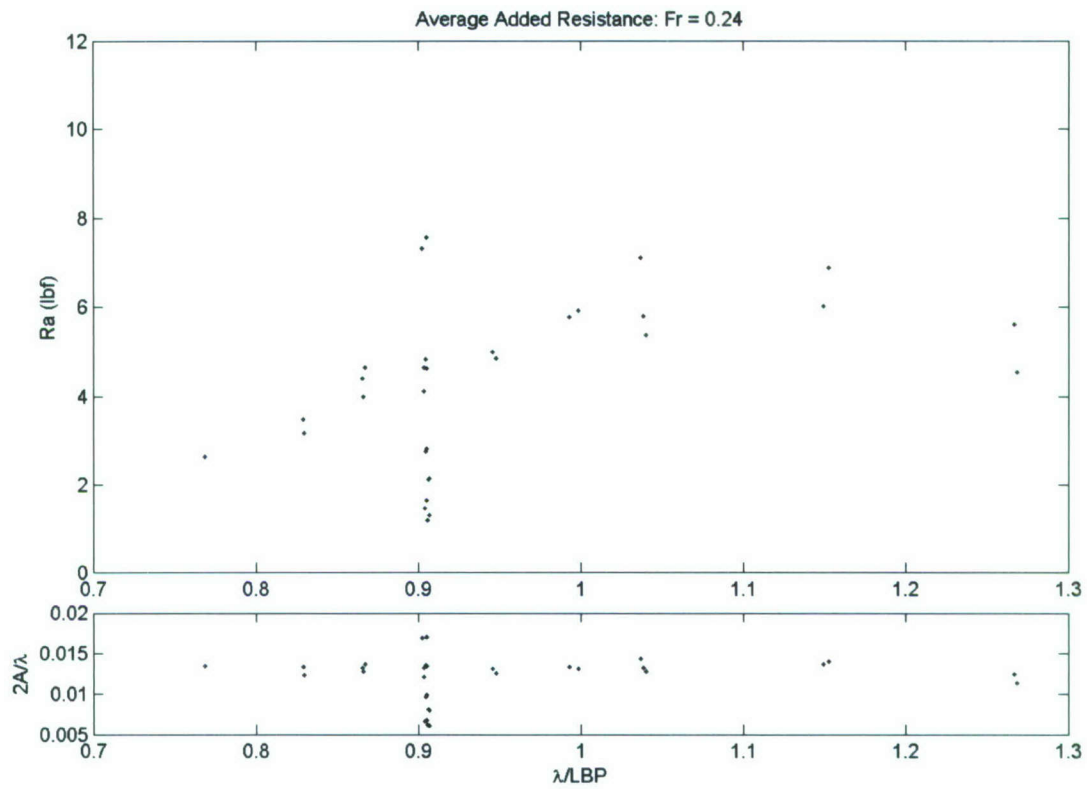


Figure 9. Average added resistance of JHSS Model 5633-3 when $Fr = 0.24$.

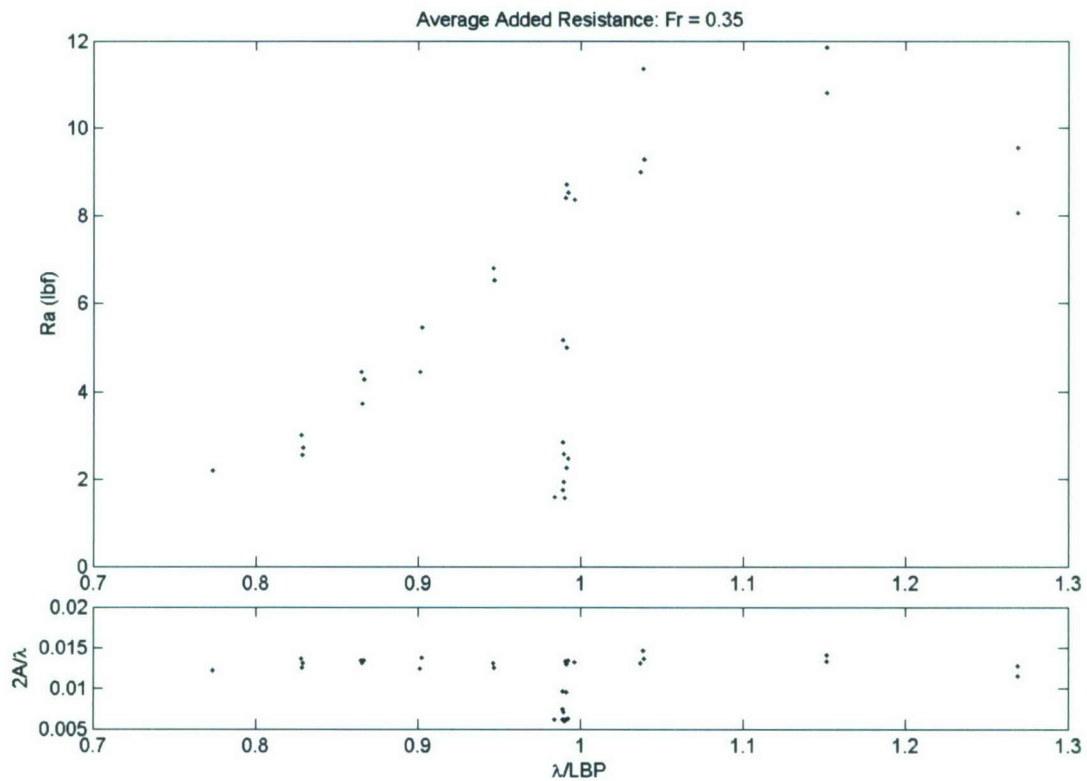


Figure 10. Average added resistance of JHSS Model 5633-3 when $Fr = 0.35$.

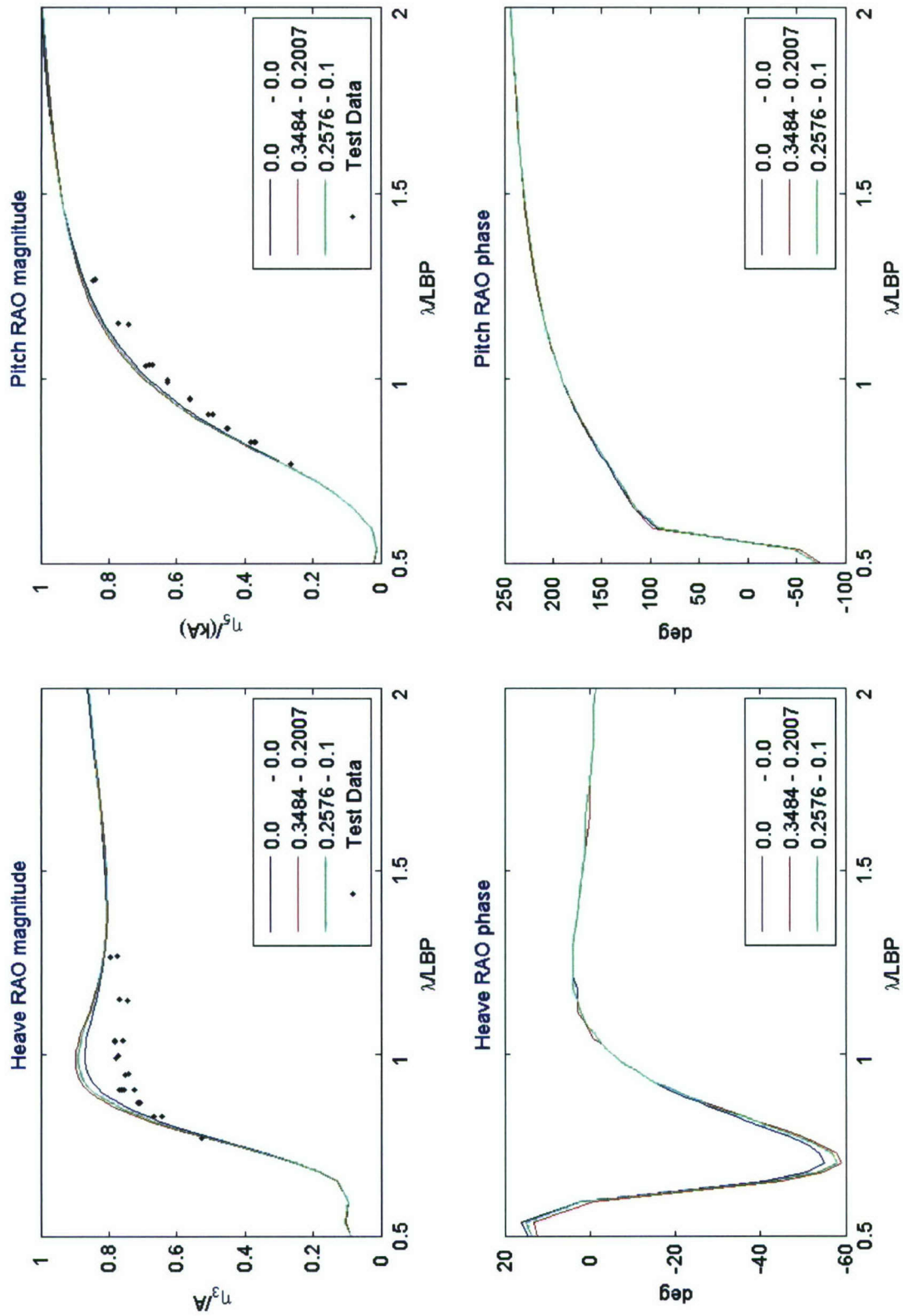


Figure 11. Heave and Pitch RAOs from SWAN1 when $Fr = 0.24$ and (sinkage, trim) = (0, 0), (0.2576 m, 0.1 deg), (0.3484 m, 0.2007 deg). Model test data were plotted with black dots.

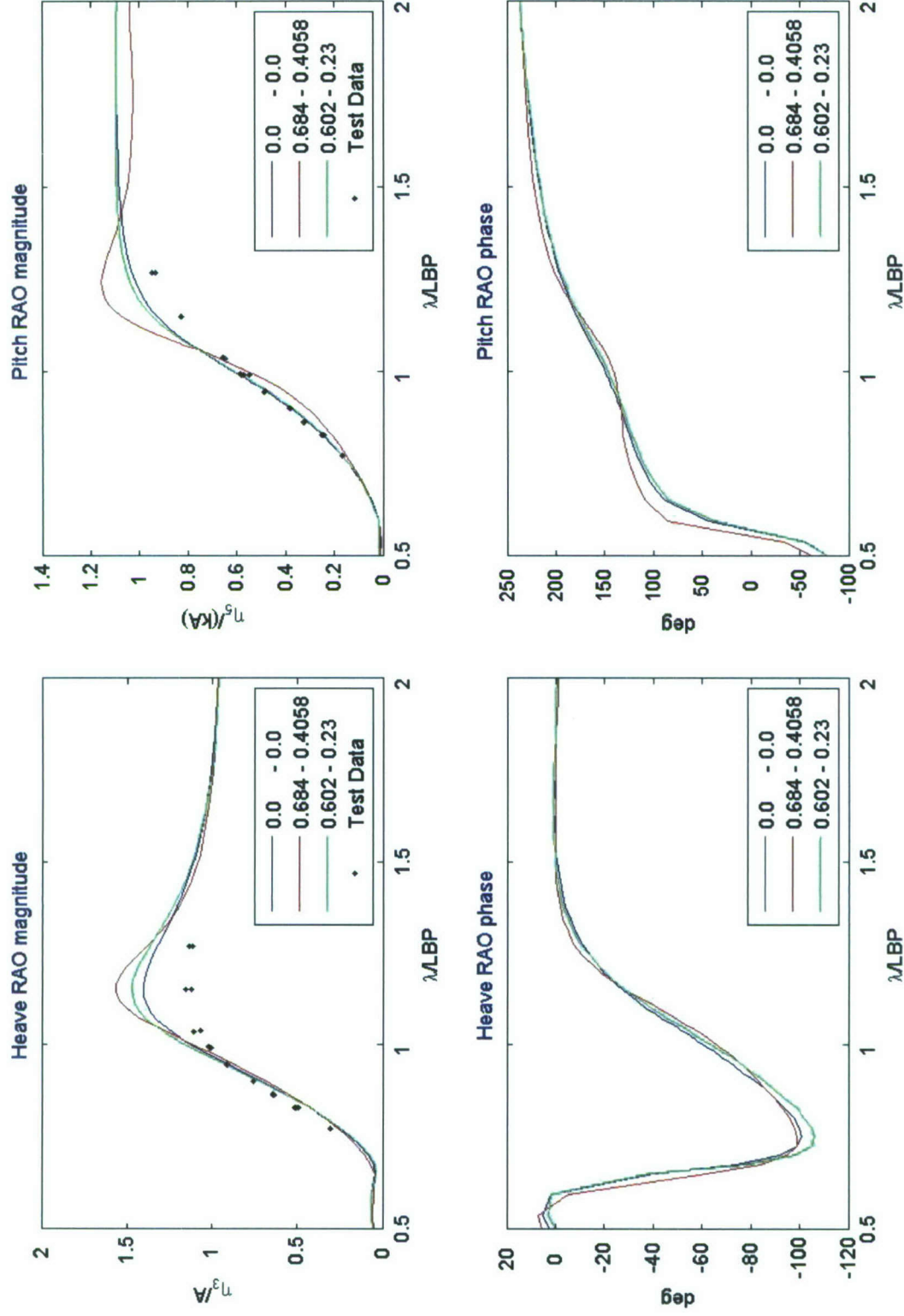


Figure 12. Heave and Pitch RAOs from SWAN1 when $Fr = 0.35$ and (sinkage, trim) = (0, 0), (0.602 m, 0.23 deg), (0.684 m, 0.4058 deg). Model test data were plotted with black dots.

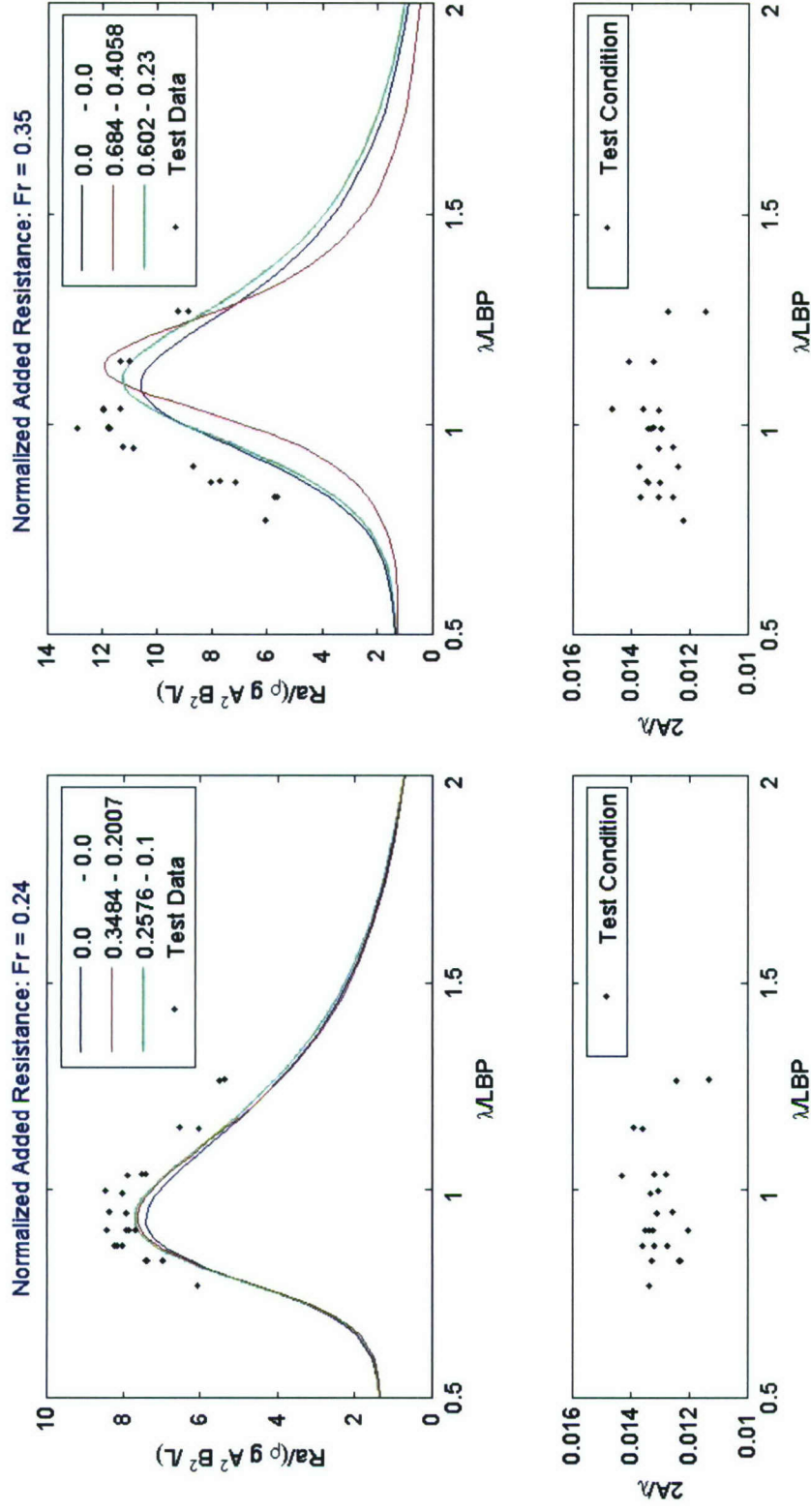


Figure 13. Normalized added resistance from SWAN1 when $Fr = 0.24$ (left) and 0.35 (right). SWAN1 results with different sinkage and trim conditions were plotted with colored lines. Model test data were plotted with black dots.

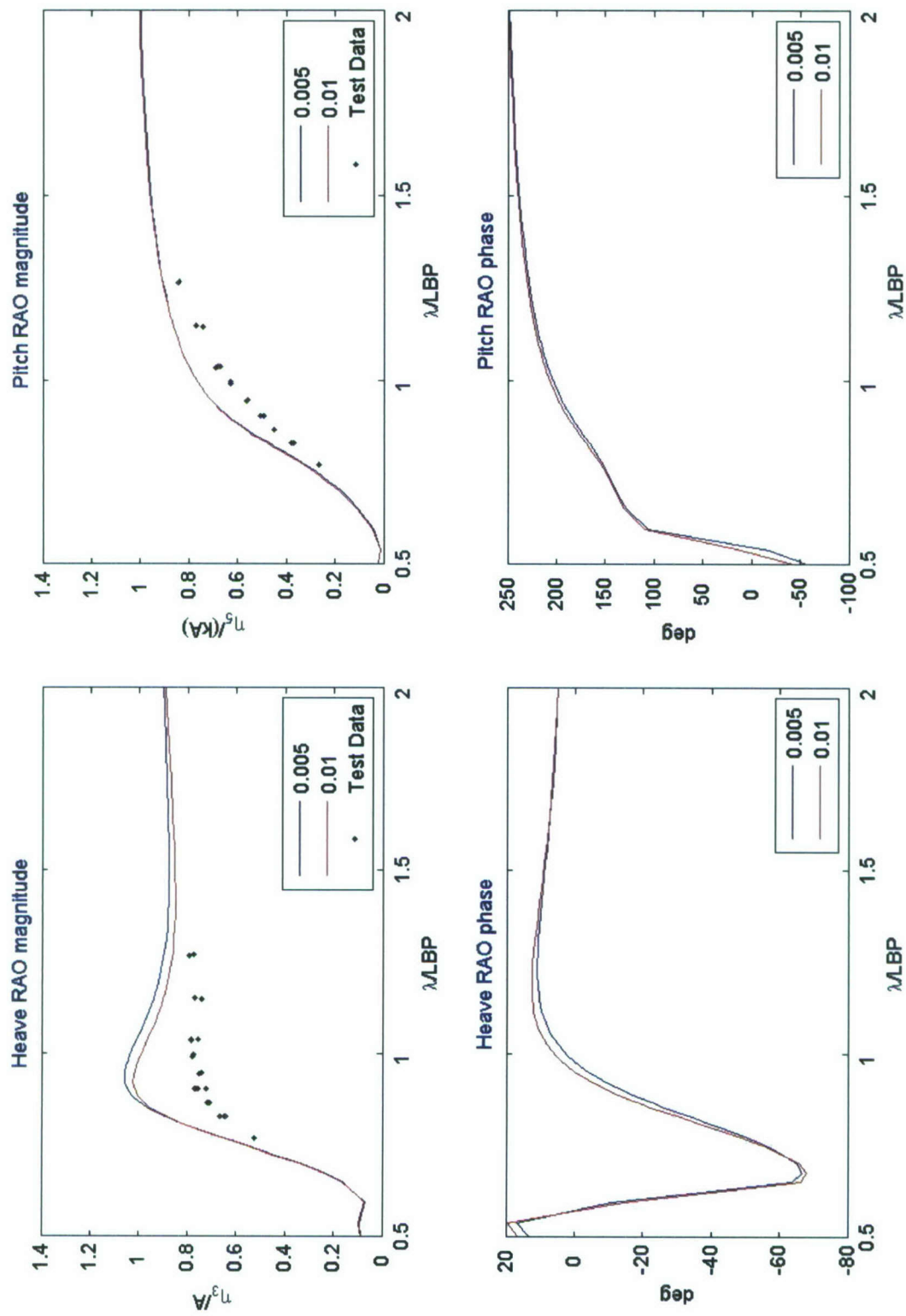


Figure 14. Heave and Pitch RAOs from LAMP2 when $Fr = 0.24$ and wave-height/wave-length = 0.005 and 0.01. Model test data were plotted with black dots.

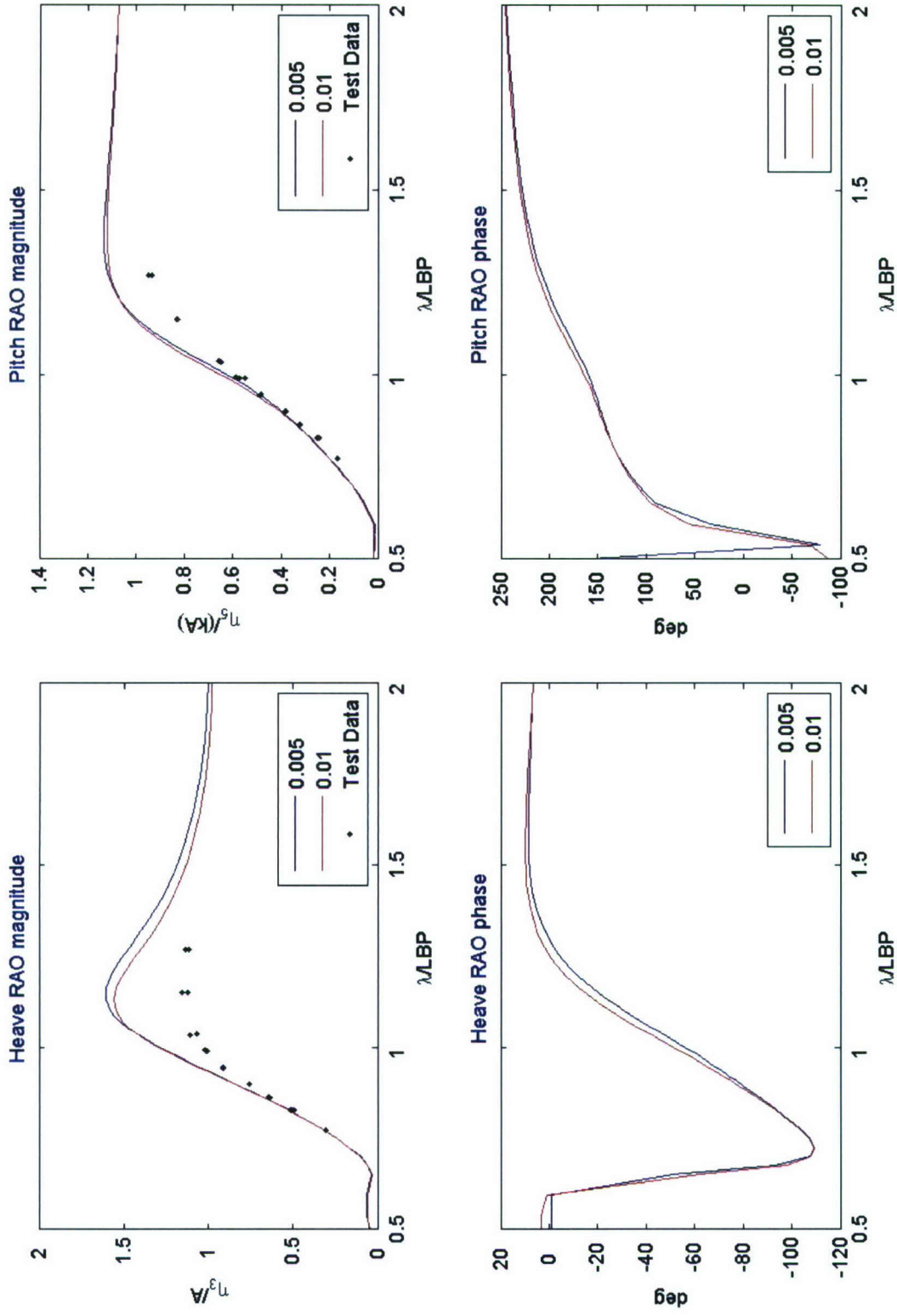


Figure 15. Heave and Pitch RAOs from LAMP2 when $Fr = 0.35$ and wave-height/wave-length = 0.005 and 0.01. Model test data were plotted with black dots

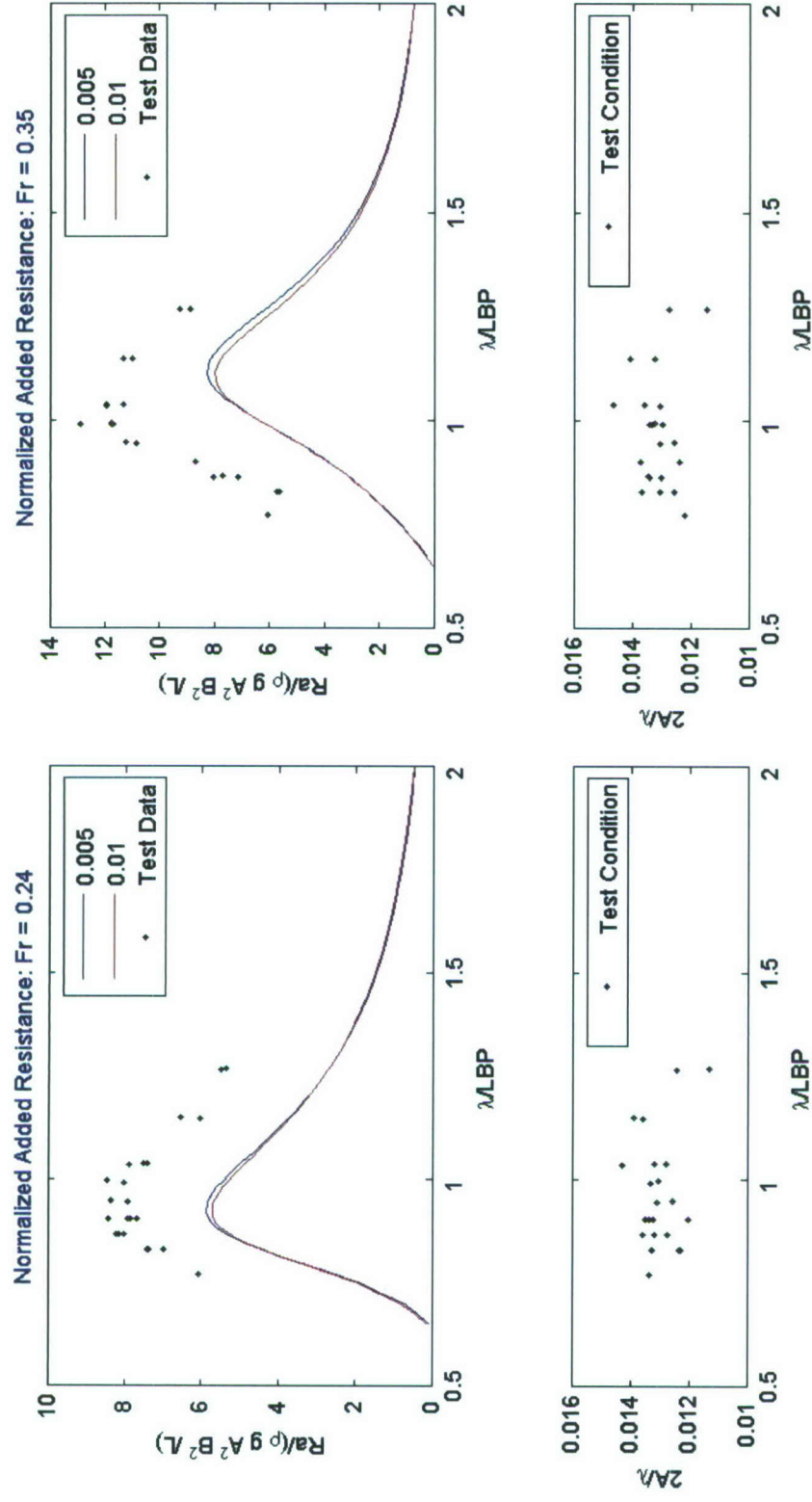


Figure 16. Normalized added resistance from LAMP2 when $Fr = 0.24$ (left) and 0.35 (right), and wave-height/wave-length = 0.005 and 0.01 . Model test data were plotted with black dots.

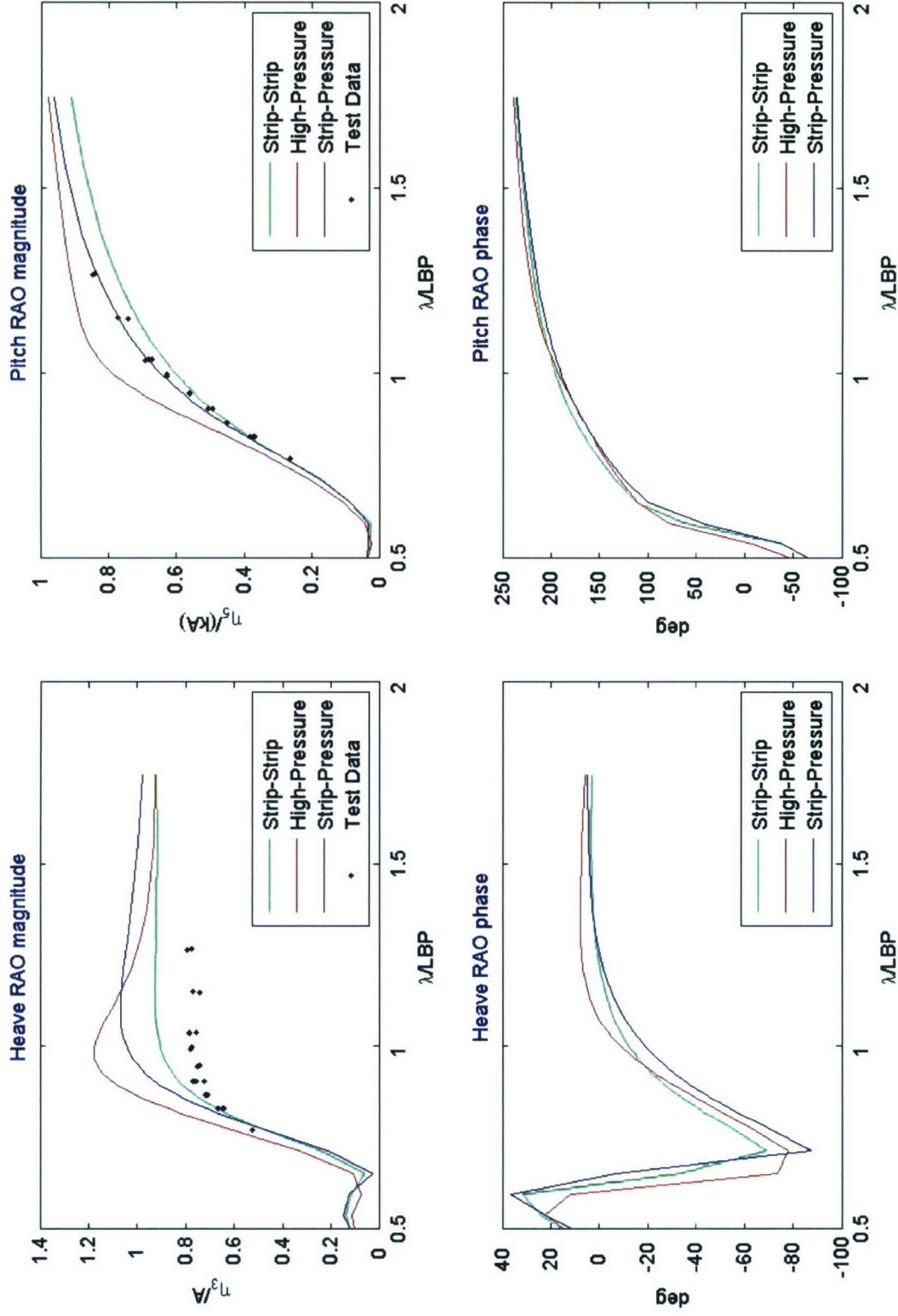


Figure 17. Heave and Pitch RAOs from VERES when $Fr = 0.24$ using different calculation methods. Strip – Strip (strip-theory formulation with strip-theory force calculation), Strip – Pressure (strip-theory formulation with pressure force integration), and High – Pressure (high-speed formulation with pressure force integration). Model test data were plotted with black dots.

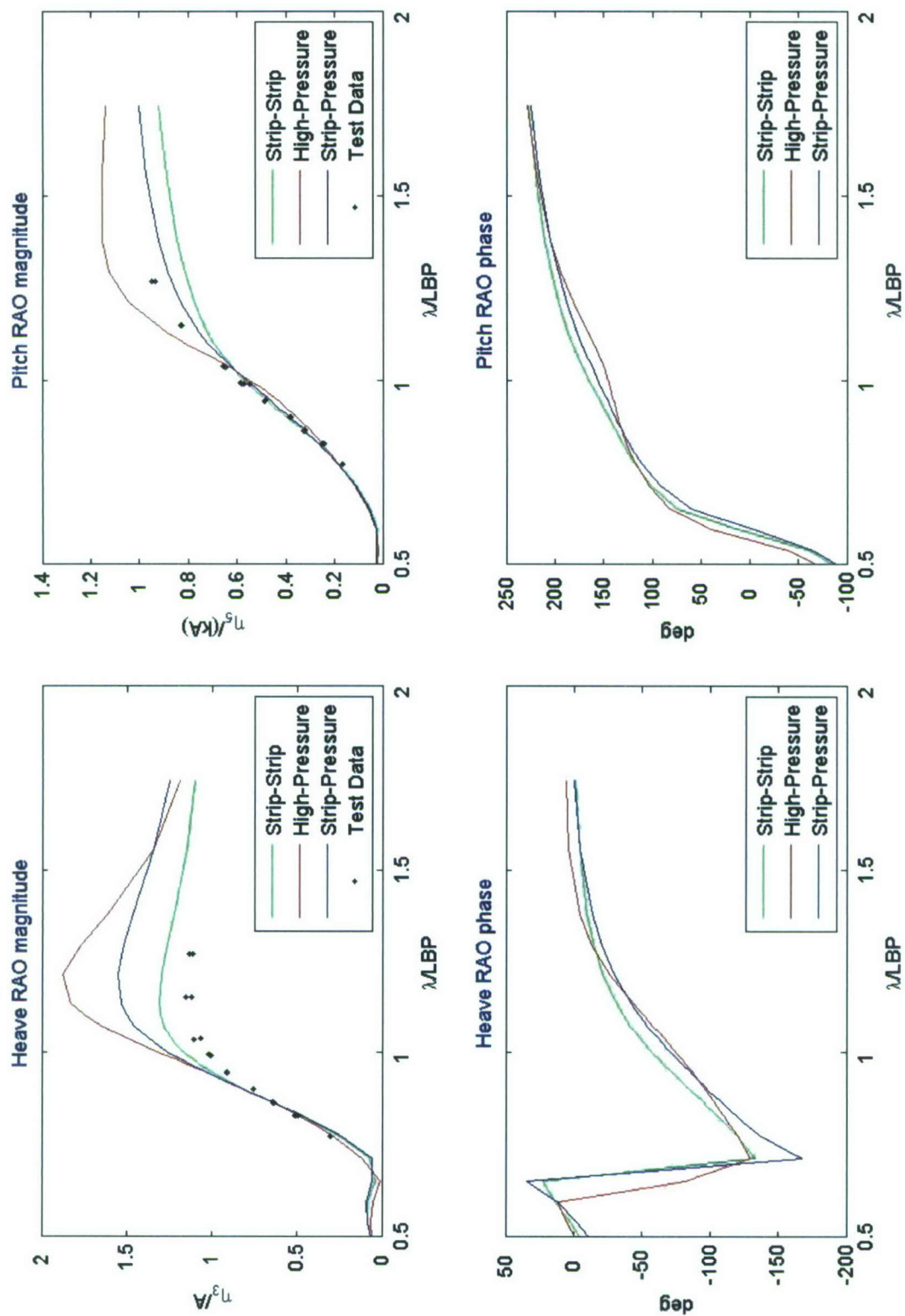


Figure 18. Heave and Pitch RAOs from VERES when $Fr = 0.35$ using different calculation methods.

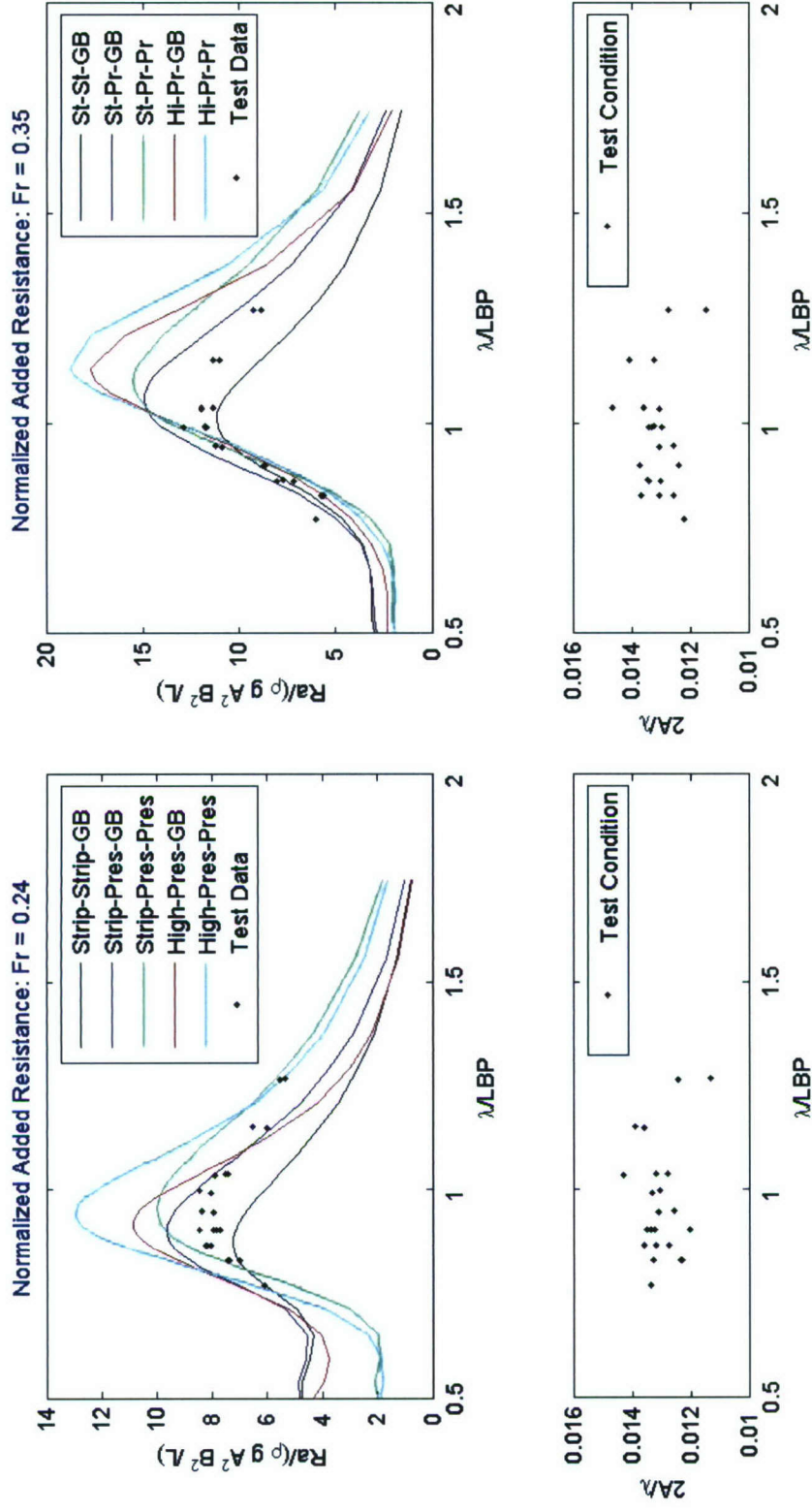


Figure 19. Normalized added resistance from VERES when $Fr = 0.24$ (left) and 0.35 (right) using different calculation methods. Strip – Strip – GB, Strip – Pressure – GB, Strip – Pressure – GB, and High – Pressure – GB. Model test data were plotted with black dots.

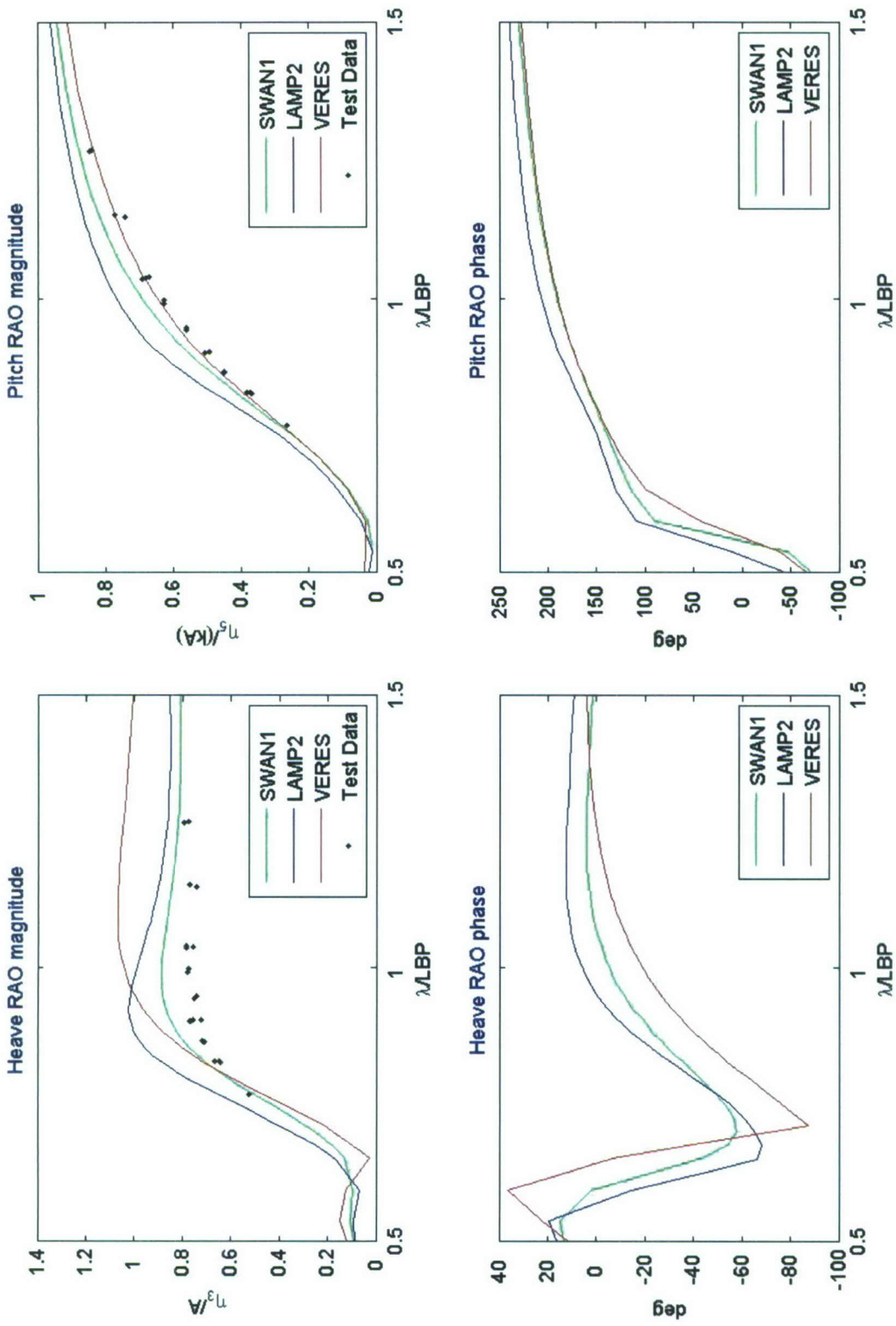


Figure 20. Comparison of Heave and Pitch RAOs between numerical predictions and model test data when $Fr = 0.24$. SWAN1 with sinkage and trim of 0.2576 m and 0.1 deg, LAMP2 with wave-height/wave-length = 0.01, and VERES with Strip – Pressure method (strip-theory formulation with pressure force integration). Model test data were plotted with black dots.

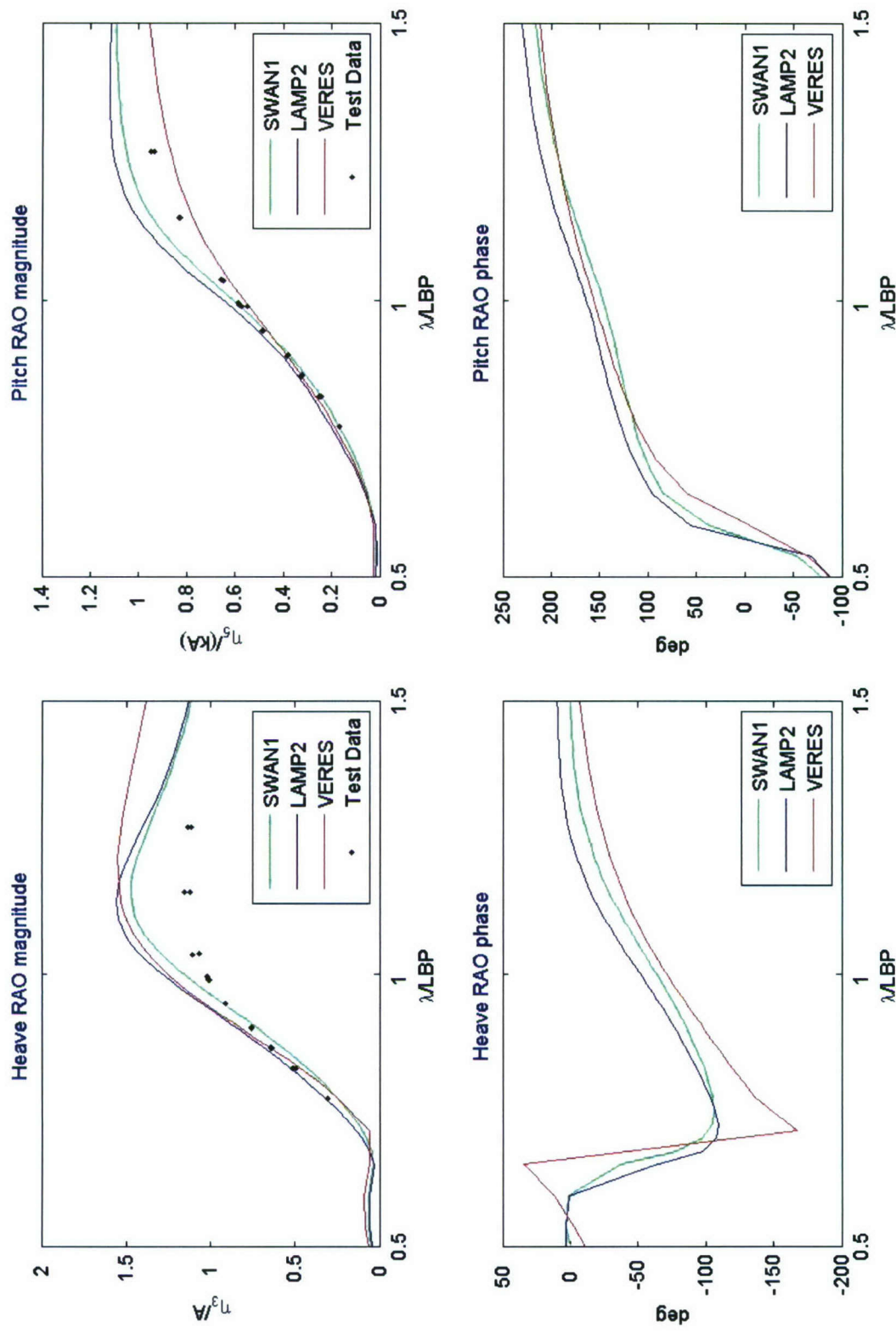


Figure 21. Comparison of Heave and Pitch RAOs between numerical predictions and model test data when $Fr = 0.35$. SWAN1 with sinkage and trim of 0.2576 m and 0.1 deg, LAMP2 with wave-height/wave-length = 0.01, and VERES with Strip – Pressure method (strip-theory formulation with pressure force integration). Model test data were plotted with black dots.

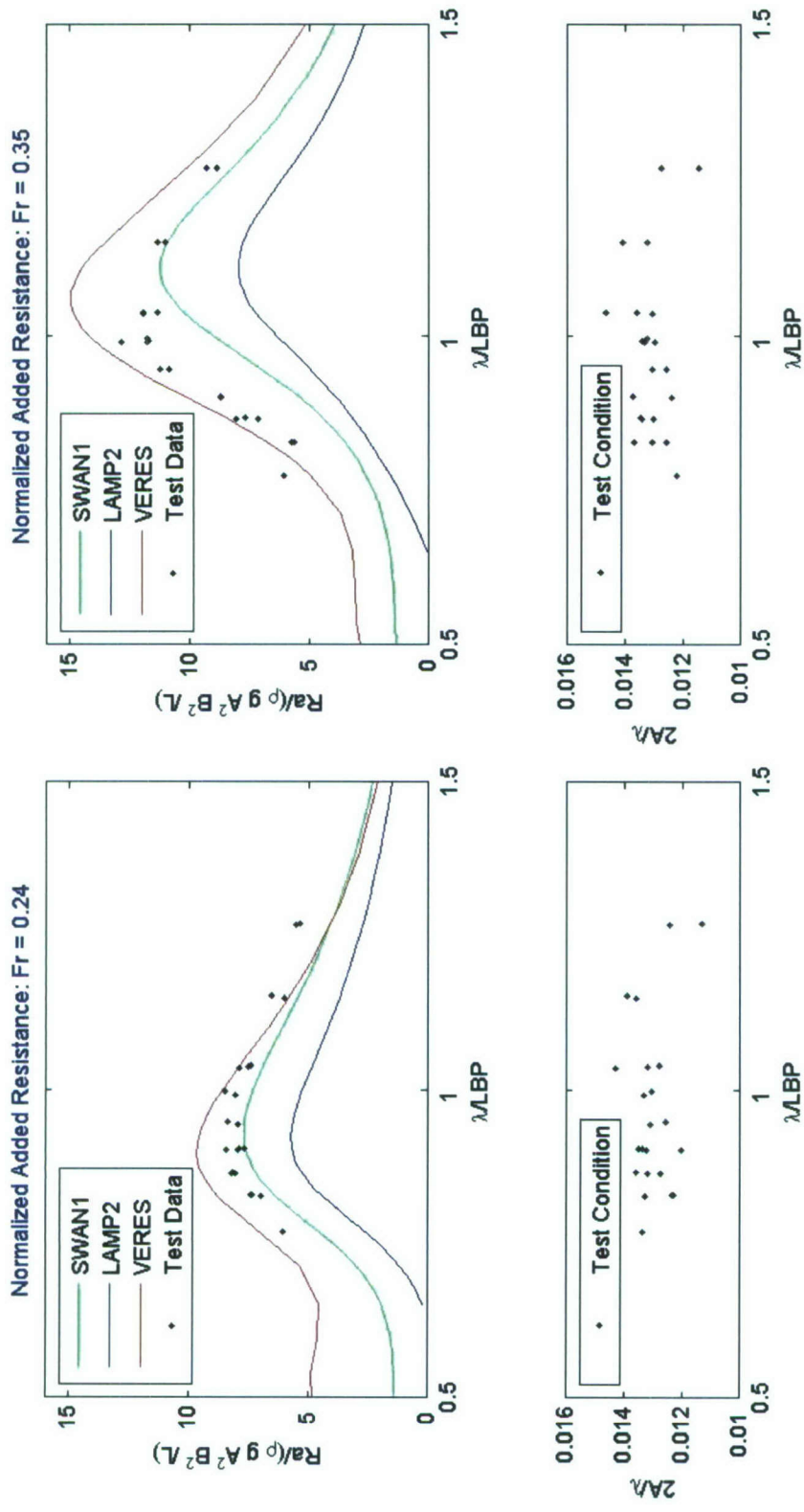


Figure 22. Comparison of normalized added resistance between numerical predictions and model test data when $Fr = 0.24$ (left) and 0.35 (right). SWAN1 with sinkage and trim of 0.2576 m and 0.1 deg, LAMP2 with wave-height/wave-length $= 0.01$, and VERES with Strip – Pressure method (strip-theory formulation with pressure force integration). Model test data were plotted with black dots.

This Page Left Intentionally Blank

REFERENCES

1. Dicks, C. A., Offutt, J. D., Anderson, R. W., & Lamb, G. R., 2007, Research & Tool Development in Support of High Speed Sealift Concepts, RINA Military Support Ships Symposium, London, Nov. 13-14, 2007, p67.
2. Strom-Tejsen, J, Yeh, Y.H. & Moran, D.D., 1973, Added Resistance in Waves, Trans. SNAME, 81, 109-143.
3. Vossers, G., 1961, Fundamentals of the Behaviour of Ships in Waves, Publication No. 151a of the Netherlands Ship Model Basin.
4. Hanaoka, T., et al, 1963, Researches on Seakeeping Qualities of Ships in Japan – Chapter 5 – Resistance in Waves, The Society of Naval Architects of Japan, 60th Anniversary Series, Vol. 8.
5. Havelock, T. H., 1942, Drifting Force on a Ship among Waves. Philosophical Magazine, Vol. 33.
6. Maruo, H., 1957, The Drift of a Body Floating on Waves. Journal of Ship Research, Vol. 4, No. 3.
7. Newman, J. N., 1967, The Drift Force and Moment on Ships in Waves. J. Ship Res., Vol. 11, pp51-60.
8. Joosen, W. P. A., 1966, Added Resistance of Ships in Waves. Proceedings of the 6th Symposium on Naval Hydrodynamics, Washington, D.C.
9. Loukakis, T. A., 1970, Computer Aided Prediction of Seakeeping Performance in Ship Design. Massachusetts Institute of Technology, Dept. of Naval Architecture and Marine Engineering, Report 70-3.
10. Gerritsma, J. & Beukelman, W., 1972, Analysis of the Resistance Increase in Waves of a Fast Cargo Ship, International Shipbuilding Progress. Vol. 19, No. 217.
11. Salvesen, N., 1974, Second-Order Steady-State Forces and Moments on Surface Ships in Oblique Regular Waves. International Symp. on the Dynamics of Marine Vehicles and Structures in Waves, Univ. of College, London, pp 212-226.
12. Lin, W. C. & Reed, A. M., 1976, The Second Order Steady Force and Moment on a Ship Moving in an Oblique Seaway. Proc. 11th Symposium on Naval Hydrodynamics, London, pp 333-351.
13. O’dea, J. F. & Kim, Y. H., 1981, Added Resistance and Power of a Frigate in Regular Waves. DTNSRDC/SPD-0964-02.
14. SWAN1 2001, Ship Flow Simulation in Calm Water and in Waves, User Manual, M. I. T.
15. User’s Guide to LAMP System, Volume I: Introduction to the LAMP System, Version 3.1.1. 2007, SAIC.
16. ShipX Vessel Response (VERES), Ship Motions and Global Loads, User’s Manual, 2004, Marintek.

17. ShipX Vessel Response (VERES), Theory Manual, 2004, Marintek
18. Salvesen, N., Tuck, E. O. & Faltinsen, O., 1970, Ship Motions and Sea Loads, Transactions of the Society of Naval Architects and Marine Engineers, Vol. 78, pp250-287.
19. Faltinsen, O. M. & Zhao, R. 1991, Numerical Predictions of Ship Motions at High Forward Speed. Phil. Trans. R. Soc. Lond. A, Vol. 334 pp 241-252.
20. Cusanelli, D. S., 2007, Joint High Speed Sealift (JHSS) Baseline Shaft & Strut (Model 5653) Series 1: Bare Hull Resistance, Appended Resistance, and Alternative Bow Evaluations. NSWCCD-50-TR-2007/066.
21. Cusanelli, D. S. & Chesnakas, C. J., 2007, Joint High Speed Sealift (JHSS) Baseline Shaft & Strut (BSS) Model 5653-3: Series 2, Propeller Disk LDV Wake Survey; and Series 3, Stock Propeller Powering and Stern Flap Evaluation Experiments. NSWCCD-50-TR-2007/084.
22. Cusanelli, D. S. & Bradel, 1994. Floating Platform Tow Post, United States Patent No. 5343742.
23. Cusanelli, D. S., 2007, Mixed-Flow Waterjet (MxWJ) Model 5662-1: Initial Study of Yaw Effects on Waterjet Powering and Transom Depth Effects on Waterjet Priming. NSWCCD-50-TR-2007/093.
24. Faltinsen, O. M., 1990, Sea Loads on Ships and Offshore Structures, Cambridge University Press.

INITIAL REPORT DISTRIBUTION

No. of Copies

Print	PDF	Office	Individual
	2	PMS 385	D. Liese, M. Fink
	1	SEA 05D1	S. Wynn
	1	SEA 05Z	R. T. Waters
	1	CSC	E. Morris
1		DTIC	

NSWCCD Code

		NSWCCD Code	Individual
	1	3452 (Library)	
	1	2000	C. Dicks
	1	2240	C. Kennell
	1	2410	A. Anderson
	2	2420	S. Fung, R. Lamb
	1	5030	S. Jessup
1		5060	D. Walden
	1	5104	S. Carpenter
			D. Cusanelli, B. Metcalf, G. Karafiath, R. Hurwitz
1	4	5800	
2		5500	Office Files
5	4	5500	S. Lee, A. Silver, T. Smith, T. Applebee
	1	6540	E. Devine

Total No. of Copies

Print	PDF
10	22